



CHALMERS

Chalmers Publication Library

Adaptive Radar Sensor Model for Tracking Structured Extended Objects

This document has been downloaded from Chalmers Publication Library (CPL). It is the author's version of a work that was accepted for publication in:

IEEE Transactions on Aerospace and Electronic Systems (ISSN: 0018-9251)

Citation for the published paper:

Hammarstrand, L. ; Lundgren, M. ; Svensson, L. (2012) "Adaptive Radar Sensor Model for Tracking Structured Extended Objects". IEEE Transactions on Aerospace and Electronic Systems, vol. 48(3), pp. 1975 - 1995.

<http://dx.doi.org/10.1109/TAES.2012.6237574>

Downloaded from: <http://publications.lib.chalmers.se/publication/161483>

Notice: Changes introduced as a result of publishing processes such as copy-editing and formatting may not be reflected in this document. For a definitive version of this work, please refer to the published source. Please note that access to the published version might require a subscription.

Chalmers Publication Library (CPL) offers the possibility of retrieving research publications produced at Chalmers University of Technology. It covers all types of publications: articles, dissertations, licentiate theses, masters theses, conference papers, reports etc. Since 2006 it is the official tool for Chalmers official publication statistics. To ensure that Chalmers research results are disseminated as widely as possible, an Open Access Policy has been adopted. The CPL service is administrated and maintained by Chalmers Library.

Adaptive radar sensor model for tracking structured extended objects

Lars Hammarstrand, Malin Lundgren, and Lennart Svensson *senior member, IEEE*

Abstract—In this paper, we propose a tracking framework jointly estimating the position of a single extended object and the set of radar reflectors that it contains. The reflectors are assumed to lie on a line structure, but the number of reflectors and their positions on the line are unknown. Additionally, we incorporate an accurate radar sensor model considering the resolution capabilities of the sensor. The evaluation of the framework on radar measurements shows promising results.

Index Terms—Radar, Sensor model, Extended targets, Tracking.

I. INTRODUCTION

HISTORICALLY, multi target radar tracking research has focused on tracking targets at large distances in the presence of clutter [1], [2]. In such scenarios, the return from a target, e.g. an aircraft, is accurately modelled as a point source, and the radar (with limited resolution) is not capable of resolving multiple features on the object. Thus it is common to assume that the object's physical extent is negligible compared to the measurement noise and that each object generates *at most* one measurement, which is known as the point source assumption.

In many other applications, such as vehicle tracking in automotive active safety systems [3], the situation is different. Here, the distance to objects is instead in the order of tens of metres and at these distances, the physical extent of objects is typically larger than the resolution of the radar sensor. Consequently, the radar is capable of resolving multiple features (reflection centres) on an object, which can lead to multiple measurements originating from the same object. The radar literature refers to these types of objects as extended targets [4]. Attempting to track this type of object using methods originally developed for point source targets will likely lead to large estimation errors as the multiple received measurements are not accurately described as originating from a point source. This is illustrated in, e.g. [3], where a detailed extended object model of radar returns from a car is compared to a simpler point source model. The extended object model provides both a better description of the vehicle-generated detections and a more accurate tracking performance compared to the point source model.

This work was sponsored by the Swedish Intelligent Vehicle Safety Systems (IVSS) program, and is a part of the SEnsor Fusion for Safety Systems (SEFS) project.

L. Hammarstrand is with Volvo Car Corporation, Gothenburg, Sweden
lhammar5@volvocars.com.

L. Hammarstrand, M. Lundgren and L. Svensson are with the Department of Signals and Systems, Chalmers University of Technology, Gothenburg, Sweden
lars.hammarstrand@chalmers.se, malin.lundgren@chalmers.se, lennart.svensson@chalmers.se

Clearly, it is possible to benefit from the fact that an object generates multiple radar measurements. In addition to a more accurate tracking it is also possible to extract more detailed information about the object, e.g., the spread of the measurements provides information about the extension and heading of the object. However, there are several difficulties that arise when tracking extended objects. For example, a considerably more complex sensor model is needed to describe the object-generated measurements with sufficient accuracy, as the measurements are spread across the whole extension of the object. Additionally, it needs to handle the situation that several features on an object might or might not be resolved by the radar sensor [5], and moreover, also describe the measurement uncertainty caused by measurements from unresolved features. The resulting tracking framework consequently, needs to treat the occurrence of possibly multiple measurements from each object, in contrast to at most one measurement in the point source case.

A comprehensive overview of the research in the area of tracking extended objects, and the closely related problem of group tracking, up to the year 2004, can be found in [6]. The PHD framework, proposed by Mahler [7], has been used extensively to address the problem of tracking groups of targets and adaptations to track extended targets are presented in [8] and [9]. In [10] and [11], Koch and Saul present a Bayesian framework for tracking an extended object or a group of closely spaced objects, under the assumption that multiple measurements can originate from the same object. The object/group extension is modelled by an elliptical shape, defined by a symmetric positive definite random matrix. This matrix is included in the state vector together with the kinematical states, and all states are jointly estimated from data. A similar model of extended objects is also in [12] but here in a combined set-theoretic and stochastic estimator. Both these models have shown to be robust against object shape but it is difficult to exploit more specific shape information if such information is available. A different approach is to model the extended object as a set of point features positioned on a (semi-) rigid structure, where each feature may be the origin of at most one measurement. This idea is adopted in, for example, [13]–[17]. However, little attention has been given to practical issues such as how to handle the uncertainties associated with limited sensor resolution or how to consider an unknown number of features on the object.

The problem of data association using possibly unresolved measurements is treated in [18] and [19], which propose two different sets of models for a joint measurement from two unresolved point sources and for the probability that the two

sources are unresolved. Using these models, the traditional data association hypotheses and measurement models are expanded to also consider merged measurements. Proposals that consider resolution uncertainty for a known but arbitrary number of sources are [3], [20]. The approach proposed in [20] is a generalised version of the probabilistic model in [19], evaluating all possible combinations of associating measurements to inter-resolved clusters of sources. In [3], the resolution uncertainty is handled by letting sources that are possibly unresolved form independent groups, where each group is capable of generating multiple measurements. In contrast to [20], the solution in [3] considers only the more probable formations of inter-resolvable sources.

In this paper, we propose a complete framework for tracking a single extended object, including estimation of both the position and kinematics of the object as well as the positions of radar reflecting features. The object is modelled, similar to [13]–[17], as (loosely) structured reflection centres sharing a common kinematic description. However, the concept is extended here to also consider uncertainty in the number of features on the structure. Additionally, we propose a radar sensor model that considers the arbitrary and unknown number of reflection centres, and which incorporates the limited resolution model presented in [20]. As a result, we are capable of adapting the description of the object-generated measurements over time as the same object might look very different to the radar depending on angle and distance. The proposed tracking framework is compared to that in [3], using data from two types of automotive radars, a 77 GHz long range radar¹ and a 24 GHz medium range radar, and the true position of the tracked vehicle is provided by an accurate differential GPS.

The paper is organised as follows. Section II introduces the notation and the problem considered in this paper. In Section III, the extended object model is presented, and Section IV describes the proposed radar sensor model in detail. A derivation of the posterior density is found in Section V while Section VI discusses how this is treated in a tracking framework. Finally, Section VII presents the results from the proposed models in a tracking framework.

Notation: To facilitate the reading of this paper, we here explain the general structure of the notation used. Vector variables are boldface, e.g. \mathbf{x} . Subscripts and superscripts in *italic* are used as indexes of some sort, e.g. time index in \mathbf{x}_k , whereas regular letters shall be interpreted as part of the variable name, e.g., P_d for the probability of detection. Regular calligraphic letters are used to indicate probabilistic events or hypotheses ($\mathcal{C}, \mathcal{D}, \mathcal{E}$) and boldface calligraphic letters ($\mathbf{\mathcal{X}}, \mathbf{\mathcal{G}}$) denote sets and graphs.

II. PROBLEM FORMULATION AND MODELLING ASSUMPTIONS

The problem that is studied in this paper is twofold: to use measurements from a radar to jointly estimate the position and kinematics of an extended object, and to adapt a structure that describes the possibly multiple radar returns from the object.

¹Long range radar in automotive applications entails a detection range of 150 m and above.

The ultimate aim is to improve the tracking of an extended object through adaptation of the radar sensor model to fit the unknown and changing behaviour of the object's radar returns.

In the coming sections we define the conditions and assumptions needed to solve this problem in a Bayesian tracking framework. The extended object model is introduced in Section II-A. In Section II-B, the radar observations are described and finally Section II-C formally defines the problem considered in the paper.

A. Extended object model

Similarly to the approach in [21], the radar return from the object of interest is assumed to be accurately modelled as originating from a set of reflection centres, i.e., a set of features on the object that are more likely to generate a strong return. The reflection centres are organised on a structure (rigid body) capturing the position, kinematics and shape of the extended object. We assume that we know that there exists one and only one visible extended object but, in contrast to [21], we assume that neither the number of reflection centres nor their initial positions are known. The information about the extended object at a discrete time instance k is summarised in an extended object state

$$\mathbf{x}_k = \left[(\mathbf{z}_k)^T, (\boldsymbol{\xi}_k)^T \right]^T. \quad (1)$$

The vector \mathbf{z}_k , called the structure state (bulk) vector, typically describes the common position and velocity of the extended object. The feature vector,

$$\boldsymbol{\xi}_k = \left[(\boldsymbol{\xi}_k^1)^T, \dots, (\boldsymbol{\xi}_k^{n_k})^T \right]^T, \quad (2)$$

contains parameters describing the positions of n_k^ξ reflection centres in relation to the structure. For a line structure, like the one in Figure 1a, $\boldsymbol{\xi}_k^i$ describes the distance (length on the structure) from the target centre to the i^{th} reflector. The position of reflection centre i in the global coordinate system is found using the mapping function $g(\mathbf{z}_k, \boldsymbol{\xi}_k^i)$. This representation can be interpreted as the positions of the reflector centres in state space being restricted to a subspace $\mathcal{S}(\mathbf{z}_k) \subseteq \mathbb{R}^{n_z}$ defined by the structure state vector \mathbf{z}_k .

Using this general description, it is possible to model different types of extended objects with a variety of imposed structures for positioning of individual reflection centres. Figure 1 shows three examples of how one can represent extended objects on the form in (1). In all the examples, the kinematic description of the object is included in the structure state vector, \mathbf{z}_k , which for the arc and box object also includes some description of the curved and rectangular shape, respectively. For the graph representation, the imposed structure is more limited and the position of the individual reflectors make up the shape of the object.

It is assumed in this paper that the time evolution of the extended object state, \mathbf{x}_k , can be divided into two parts,

$$\mathbf{x}_{k+1} = \begin{bmatrix} \mathbf{z}_{k+1} \\ \boldsymbol{\xi}_{k+1} \end{bmatrix} = \begin{bmatrix} f_z(\mathbf{x}_k, \mathbf{v}_k^z) \\ f_\xi(\mathbf{x}_k, \mathbf{v}_k^\xi) \end{bmatrix}, \quad (3)$$

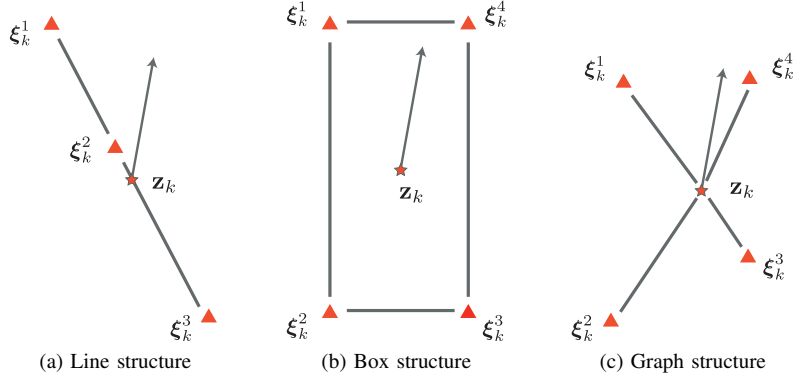


Figure 1. Different structure model alternatives for representing an extended object. Example (a) models the extended object as a line with the reflectors positioned along it, example (b) as a rectangle and example (c) as a more general graph shape.

where $f_z(\cdot)$ describes the dynamic behaviour of the structure and $f_\xi(\cdot)$ captures the dynamics of the reflector centres in relation to the structure and the change in the number of reflectors. The variables, \mathbf{v}_k^z and \mathbf{v}_k^ξ , are noise process accounting for model uncertainties.

B. Radar observations

Observations on the positions of the reflection centres are provided by radar sensors mounted on a possibly moving host platform, and it is assumed that both the position of the sensors and the state of the host platform, denoted \mathbf{z}_k^h , are known parameters in the measurement model. The sensors are similar in that if a feature on the extended object is a strong scatterer for one sensor, this is also true for the others. At each time k , only one of the radar sensors provides a set of measurements, and as a result, although we have a multi-sensor system, we only need to consider measurements from one sensor at each update step. All sensors are thus treated separately and in a similar manner and to simplify notation, the presentation is limited to one of the sensors.

At each time instance k , a sensor provides M_k detections, where m_k^t detections are generated by the extended object and m_k^c observations are clutter. All detections are stored in the unlabelled measurement vector,

$$\mathbf{y}_k = \left[(\mathbf{y}_k^1)^T, (\mathbf{y}_k^2)^T, \dots, (\mathbf{y}_k^{M_k})^T \right]^T. \quad (4)$$

Each measurement in (4) contains an observation of the relative range, r_k^i , angle, ϕ_k^i , and range rate, \dot{r}_k^i , between one radar reflection source (object related or clutter) and the sensor, such that

$$\mathbf{y}_k^i = [r_k^i, \phi_k^i, \dot{r}_k^i]^T. \quad (5)$$

The collection of all measurement vectors up to and including time instance k is denoted $\mathbf{Y}_k \triangleq \{\mathbf{y}_1, \mathbf{y}_2, \dots, \mathbf{y}_k\}$.

Let us define an ordered collection of the detections which originate from the extended object and those which originate from clutter as

$$\mathbf{y}_k^t = \left[\left(\mathbf{y}_k^{t,1} \right)^T, \dots, \left(\mathbf{y}_k^{t,m_k^t} \right)^T \right]^T \quad (6)$$

$$\mathbf{y}_k^c = \left[\left(\mathbf{y}_k^{c,1} \right)^T, \dots, \left(\mathbf{y}_k^{c,m_k^c} \right)^T \right]^T. \quad (7)$$

These two vectors are connected to the measurement vector, \mathbf{y}_k , through an unknown random permutation matrix, $\Pi_p^{M_k}$, with dimension $[M_k \times M_k]$. This relation can mathematically be expressed as

$$\mathbf{y}_k = (\Pi_p^{M_k} \otimes \mathbf{I}_{3 \times 3}) \begin{bmatrix} \mathbf{y}_k^c \\ \mathbf{y}_k^t \end{bmatrix}, \quad (8)$$

where \otimes is the Kronecker product and $\mathbf{I}_{3 \times 3}$ is a three-by-three-dimensional identity matrix. The purpose of $\Pi_p^{M_k}$ is to describe the uncertainty in measurement origin (data association uncertainty). The treatment of this uncertainty is an important part in the derivation of the tracking framework, and is further discussed in Section VI.

The clutter measurement vector, \mathbf{y}_k^c , is assumed to behave according to a known and object-independent clutter model describing both the number of clutter detections m_k^c and their spatial distribution. The m_k^t object-generated detections are naturally described by the reflection centres on the structure. Given a state vector \mathbf{x}_k with N_k^ξ reflectors², the positions of these reflectors in the observation space, denoted \mathbf{r}_k , and the parameter describing the expected return signal amplitude from the reflectors, denoted σ_k , are given by a known function

$$[(\mathbf{r}_k)^T, (\sigma_k)^T]^T = h_\xi(\mathbf{x}_k) \quad (9)$$

where $\mathbf{r}_k = [(\mathbf{r}_k^1)^T, \dots, (\mathbf{r}_k^{N_k^\xi})^T]^T$ and $\sigma_k = [\sigma_k^1, \dots, \sigma_k^{N_k^\xi}]^T$. Under ideal conditions, the object measurement vector, \mathbf{y}_k^t , would contain one detection from each reflection centre, i.e., $\mathbf{y}_k^{t,i} = \mathbf{r}_k^i$. However, due to limitations in radar signal bandwidth and pulse duration as well as antenna aperture size, radar sensors are not capable of resolving reflection centres that are too closely spaced. As such, all reflectors are not always resolvable and the response from a cluster of reflectors might merge to form a joint detection. Additionally, a reflector or a cluster of reflectors will be detected only if the signal to noise ratio of its radar return is sufficiently large. We assume that the object measurements from a reflector or a cluster of reflectors can be described as

$$\mathbf{y}_k^t = h_c(\mathbf{r}_k, \sigma_k, \mathbf{w}_k), \quad (10)$$

²Conditioned on \mathbf{x}_k , the number of reflection centres is known. This is indicated by denoting the number of reflectors using uppercase N instead of lowercase.

where $h_c(\cdot)$ is a stochastic function and \mathbf{w}_k is a measurement noise process capturing both model uncertainties and measurement disturbances. The function $h_c(\cdot)$ describes m_k^t detections from inter-resolved reflector clusters and is stochastic in the sense that it changes depending on how the n_k^ξ reflectors are partitioned into resolvable reflector clusters, and which of the clusters that are detected by the sensor.

C. Tracking problem

As aforementioned, the aim of this paper is to derive a Bayesian tracking framework for jointly estimating the structure state, \mathbf{z}_k , as well as the number of reflection centres, n_k^ξ , and their positions, ξ_k , on the extended object, based on noisy radar observations, \mathbf{Y}_k . As new measurements are available, the posterior density, $p(\mathbf{x}_k | \mathbf{Y}_k)$, is recursively calculated. From this density it is possible to compute estimates including uncertainty measures under different optimality constraints.

For the type of problem considered in this paper, the calculation of $p(\mathbf{x}_k | \mathbf{Y}_k)$ is feasible using knowledge from two types of probabilistic models: the process model defined by (3) and the measurement model defined in (8). Furthermore, we need to consider three additional types of uncertainties influencing our ability to interpret the measurements. First, we need to handle that the number of reflection centres on the structure is unknown and time-varying (existence uncertainty). Second, even under known number of reflection centres, the object measurement model (10) is stochastic due to uncertainty regarding how the reflectors are partitioned into inter-resolvable reflector clusters (resolution uncertainty). Finally, we do not know which of the clusters that are detected by the sensor and which of the measurements in \mathbf{y}_k corresponds to which object detection (data association uncertainty).

These aspects of the calculation of the posterior density are addressed in the following sections. In Section III, we define the parametrisation of the extended object considered in this paper, together with the process model (3). The radar sensor model which incorporates resolution uncertainty is derived in Section IV. By introducing interdependent hypotheses to handle the *existence, cluster and data association uncertainties* with associated probabilistic models, the derivation of the posterior density based on the process and radar sensor model is concluded in Section V. The existence, cluster and data association hypotheses indicate which reflectors on the object exists, which of these form inter-resolvable clusters and which measurement originated from which cluster, respectively. Finally, to arrive at a more computational tractable solution, we marginalise over the hypotheses and introduce suitable approximations in Section VI.

III. STRUCTURE MODEL

This section describes the specific extended object model used in this paper, i.e., a structure to which a collection of reflector centres are attached. We will discuss the state parametrisation of the extended object as well as models for its evolution over time. This includes both the motion of the structure and the reflection centres, as well as how the number of reflectors changes over time.

A. Structure parametrisation

In this paper we propose to use a simple yet useful structure model. We assume that an extended object can be modelled as a straight line to which the unknown number of reflector centres are associated, as shown in Figure 2. All parameters of interest for describing this structure are collected in a discrete time state vector, \mathbf{x}_k . As in [21], this vector consists of two parts, namely a structure state vector \mathbf{z}_k containing, e.g., the position, velocity and heading of the line, and a feature vector, ξ_k , describing the positions of the reflector centres on the structure.

The state vector for the line structure in this paper is parameterised as

$$\mathbf{z}_k = [x_k, y_k, \psi_k, v_k, c_k, a_k, \theta_k]^T, \quad (11)$$

where (x_k, y_k) is defined as the mid point as well as the rotation point of the line, and is expressed in global Cartesian coordinates. The rotation point travels at an instantaneous speed v_k and acceleration a_k in the direction of travel described by the heading angle ψ_k . Further, the heading and the line rotates along the trajectory described by the curvature c_k ³, and the line itself is rotated relative to its heading according to θ_k .

The feature vector ξ_k , that describes the reflector positions on the structure, is defined as

$$\xi_k = [l_k^1, l_k^2, \dots, l_k^{n_k^\xi}]^T, \quad (12)$$

where n_k^ξ is the unknown (and stochastic) number of reflectors, and l_k^i is the distance from the line centre to the i^{th} reflector. The complete extended object state vector is $\mathbf{x}_k = [\mathbf{z}_k^T, l_k^1, l_k^2, \dots, l_k^{n_k^\xi}]^T$.

B. Structure process model

The structure state evolves over time according to the time-continuous motion model

$$\dot{\mathbf{z}}(t) = \begin{bmatrix} v(t)\cos(\psi(t)) \\ v(t)\sin(\psi(t)) \\ c(t)v(t) \\ a(t) \\ 0 \\ 0 \\ 0 \end{bmatrix} + \begin{bmatrix} 0 \\ 0 \\ 0 \\ 0 \\ \nu_c(t) \\ \nu_a(t) \\ \nu_\theta(t) \end{bmatrix}, \quad (13)$$

where ν_c , ν_a and ν_θ are white time-continuous zero-mean Gaussian noise processes with variances σ_c^2 , σ_a^2 and σ_θ^2 , respectively. A discrete-time version of (13) is readily available on the form

$$\mathbf{z}_k = f_z(\mathbf{z}_{k-1}) + \mathbf{v}_k^z \quad (14)$$

derived assuming constant noise increments during one sampling period, and where $\mathbf{v}_k^z \sim \mathcal{N}(\mathbf{0}, \mathbf{Q}_z)$ is the corresponding discrete time noise process. The exact expression of (14) is not given here for brevity, but the interested reader can find the discrete time version of a similar model in [3].

³The curvature c_k is here used to describe the heading change rate of the line structure as a function of distance. Definition: The rotation point travels on the circumference of a circle with radius $1/c_k$ (see Fig. 2).

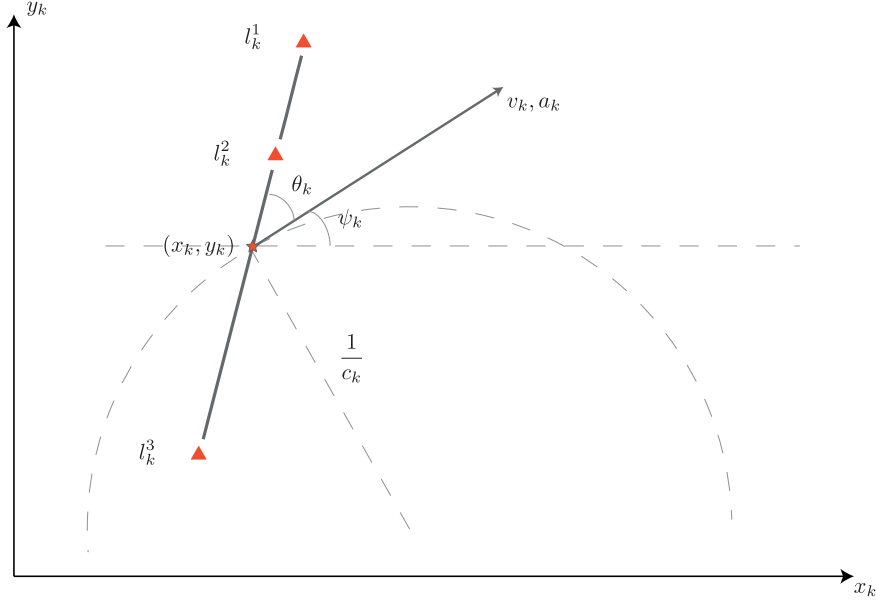


Figure 2. In this paper an extended object is modelled as a line to which a collection of reflection centres is associated. The state vector, \mathbf{z}_k , describing the structure is parameterised in a global Cartesian coordinate system.

C. Feature process model

The process model for the feature state, as defined in (3), needs both to describe how the reflectors move on the structure, and account for changes in the number of reflectors. The number of reflectors can change in part due to existing reflectors disappearing and in part due to new reflectors appearing. Let us assume that the feature process model can be partitioned as

$$\xi_k = \begin{bmatrix} \xi_k^s \\ \xi_k^b \end{bmatrix} = \begin{bmatrix} f_\xi^s(\mathbf{x}_{k-1}, \mathbf{v}_{k-1}^s) \\ f_\xi^b(\mathbf{x}_{k-1}, \mathbf{v}_k^b) \end{bmatrix}, \quad (15)$$

where ξ_k^s and ξ_k^b are random vectors containing the positions of the n_k^s surviving reflectors from time $k-1$ and the n_k^b appearing reflectors at time k . Both n_k^s and n_k^b are assumed unknown and random and the respective feature vector is modelled by the survival process model $f_\xi^s(\cdot)$ and the birth process model $f_\xi^b(\cdot)$. The noise processes, \mathbf{v}_{k-1}^s and \mathbf{v}_k^b , describe uncertainties in the dynamics of the surviving reflectors and in the position of born reflectors.

1) *Survival model:* To indicate whether reflector i in ξ_{k-1} is still present at time k (survives until time k) or not, we introduce an existence (survival) variable $e_{s,k}^i \in \{0, 1\}$, where $e_{s,k}^i = 1$ indicates that the i^{th} reflector survived and vice versa for $e_{s,k}^i = 0$. Further, we denote $P_{s,k}^i = \Pr\{e_{s,k}^i = 1 | \xi_{k-1}\}$ and $1 - P_{s,k}^i$ as the probability of the respective outcome. Let the survival hypothesis, denoted \mathcal{E}_k^s , indicate one possible ordered set of N_k^s surviving reflectors, $\{s_1, \dots, s_{N_k^s}\} = \{i : e_{s,k}^i = 1\}$, such that $1 \leq s_1 < \dots < s_{N_k^s} \leq N_{k-1}^s$. Using this hypothesis, the survival process model is modelled as a simple random walk,

$$\xi_k^s = f_\xi^s(\xi_{k-1}, \mathcal{E}_k^s, \mathbf{v}_{k-1}^s) = \begin{bmatrix} l_{k-1}^{s_1} \\ \vdots \\ l_{k-1}^{s_{N_k^s}} \end{bmatrix} + \begin{bmatrix} \mathbf{v}_{k-1}^{s,s_1} \\ \vdots \\ \mathbf{v}_{k-1}^{s,s_{N_k^s}} \end{bmatrix}, \quad (16)$$

where $\mathbf{v}_{k-1}^{s,i} \sim \mathcal{N}(0, \sigma_s^2)$ is a noise process included to allow for a small movement of a reflector along the line structure.

From the survival model, the transition density for ξ_k^s can be formed as

$$p(\xi_k^s | \xi_{k-1}) = \sum_{\mathcal{E}_k^s} p(\xi_k^s | \mathcal{E}_k^s, \xi_{k-1}) \Pr\{\mathcal{E}_k^s | \xi_{k-1}\} \quad (17)$$

where

$$p(\xi_k^s | \mathcal{E}_k^s, \xi_{k-1}) = \prod_{j=1}^{N_k^s} \mathcal{N}(l_k^j; l_{k-1}^{s_j}, \sigma_s^2) \quad (18)$$

$$\Pr\{\mathcal{E}_k^s | \xi_{k-1}\} = \prod_{i=1}^{N_{k-1}^s} (1 - P_{s,k}^i) \prod_{j=1}^{N_k^s} \frac{P_{s,k}^{s_j}}{1 - P_{s,k}^{s_j}}. \quad (19)$$

2) *Birth model:* At a time k , we assume that a maximum number of B_k new reflectors appear on the structure, each with a position described by a Gaussian density $l_k^{b,i} \sim \mathcal{N}(l_k^{b,i}, \sigma_b^2)$. Again, we introduce an existence variable, $e_{b,k}^i \in \{0, 1\}$ stating whether reflector i is born or not and denote the corresponding birth probability as $P_{b,k}^i$. Similarly as in the survival process, we let a birth hypothesis \mathcal{E}_k^b indicate one possible ordered set of N_k^b appearing reflectors, $\{b_1, \dots, b_{N_k^b}\} = \{i : e_{b,k}^i = 1\}$, such that the birth process can be written as

$$\xi_k^b = f_\xi^b(\mathcal{E}_k^b, \mathbf{v}_k^b) = \begin{bmatrix} l_k^{b,b_1} \\ \vdots \\ l_k^{b,b_{N_k^b}} \end{bmatrix} + \begin{bmatrix} \mathbf{v}_k^{b,b_1} \\ \vdots \\ \mathbf{v}_k^{b,b_{N_k^b}} \end{bmatrix}, \quad (20)$$

where $\mathbf{v}_k^{b,b_i} \sim \mathcal{N}(0, \sigma_b^2)$. Using (20), the pdf of ξ_k^b can be formed as

$$p(\xi_k^b) = \sum_{\mathcal{E}_k^b} p(\xi_k^b | \mathcal{E}_k^b) \Pr\{\mathcal{E}_k^b\} \quad (21)$$

where

$$p(\xi_k^b | \mathcal{E}_k^b) = \prod_{j=1}^{N_k^b} \mathcal{N}(l_k^j; l_k^{b,b_j}, \sigma_b^2) \quad (22)$$

$$\Pr\{\mathcal{E}_k^b\} = \prod_{j=1}^{B_k} \left(1 - P_{b,k}^j\right) \prod_{j=1}^{N_k^b} \frac{P_{b,k}^{b_j}}{1 - P_{b,k}^{b_j}}. \quad (23)$$

D. Extended object process model

Through forming an existence hypothesis, $\mathcal{E}_k = \{\mathcal{E}_k^s, \mathcal{E}_k^b\}$, and using the process models for the structure and the reflector centres, the complete process model for the extended object, conditioned on the existence hypothesis, can be stated

$$\mathbf{x}_k = f(\mathbf{x}_{k-1}, \mathcal{E}_k, \mathbf{v}_{k-1}) = \begin{bmatrix} f_z(\mathbf{z}_{k-1}) + \mathbf{v}_{k-1}^z \\ f_\xi^s(\xi_{k-1}, \mathcal{E}_k^s, \mathbf{v}_{k-1}^s) \\ f_\xi^b(\mathcal{E}_k^b, \mathbf{v}_k^b) \end{bmatrix}. \quad (24)$$

The corresponding conditional transition density can be expressed as

$$\begin{aligned} p(\mathbf{x}_k | \mathcal{E}_k, \mathbf{x}_{k-1}) &= \mathcal{N}(\mathbf{z}_k; f_z(\mathbf{z}_{k-1}), \mathbf{Q}_z) \times \\ &\prod_{j=1}^{N_k^s} \mathcal{N}(l_k^j; l_k^{s_j}, \sigma_s^2) \prod_{j=N_k^s+1}^{N_k^s+N_k^b} \mathcal{N}(l_k^j; l_k^{b,b_j}, \sigma_b^2) \\ &\triangleq \mathcal{N}(\mathbf{x}_k; \bar{\mathbf{x}}_k^\mathcal{E}, \mathbf{Q}_k^\mathcal{E}), \end{aligned} \quad (25)$$

where $\bar{\mathbf{x}}_k^\mathcal{E} = f(\mathbf{x}_{k-1}, \mathcal{E}_k, \mathbf{0})$ is the deterministic part of (24), and $\mathbf{Q}_k^\mathcal{E}$ is the process noise covariance. The transitional existence hypothesis probability is found as $\Pr\{\mathcal{E}_k | \xi_{k-1}\} = \Pr\{\mathcal{E}_k^s | \xi_{k-1}\} \Pr\{\mathcal{E}_k^b\}$.

IV. RADAR SENSOR MODEL

The objective of this section is to present the radar sensor model for the clutter measurement vector, \mathbf{y}_k^c , and the object measurement vector, \mathbf{y}_k^t , in (8) given an extended object state vector \mathbf{x}_k . Recall that \mathbf{x}_k includes both the structure state as well as the number of reflectors and their positions on the structure. From \mathbf{y}_k^c and \mathbf{y}_k^t it is then possible to form the measurement vector, \mathbf{y}_k , by generating a random permutation matrix $\Pi_p^{M_k}$.

For the clutter measurements we adopt the assumption that \mathbf{y}_k^c is described by a homogenous Poisson process in the observation space according to

$$\mathbf{y}_k^{c,i} \sim \text{Uniform}(V), \quad (26)$$

$$m_k^c \sim \text{Poisson}(\mu V), \quad (27)$$

where $\mathbf{y}_k^{c,i}$ is the i^{th} clutter measurement, μ is the clutter intensity and V the volume of the observation space. In addition, we assume that the clutter detections are independent from each other and from the object detections.

Under ideal conditions the object measurement vector, \mathbf{y}_k^t , would contain one detection from each reflection centre, and the vector $\mathbf{y}_k^{t,i}$ would be the corresponding reflector position in observation space as defined in (9). However, due to measurement noise, limited sensor resolution and a probability of detection less than one, the situation is not that simple.

To start with, the exact physical model for determining which reflectors that are resolved and which are clustered, i.e. unresolved, is not easily derived. For this reason, we resort to a stochastic description of the phenomenon based on evaluating all possible cluster formations. Given a state vector \mathbf{x}_k , a cluster formation is a partitioning of the N_k^c reflectors in ξ_k into a set of inter-resolvable clusters of reflectors, i.e., the returns from reflectors in a cluster are unresolvable to the radar while the radar is capable of distinguishing returns from reflectors in different clusters. Let a cluster hypothesis \mathcal{C}_k indicate one of these formations and let the probability of \mathcal{C}_k be modelled by $\Pr\{\mathcal{C}_k | \mathbf{x}_k\}$. The resolution capabilities of a sensor can thus be probabilistically described by generating all possible cluster formations and evaluating their probabilities using $\Pr\{\mathcal{C}_k | \mathbf{x}_k\}$.

Under a given cluster hypothesis, it is assumed that each cluster in the formation can generate at most one detection. This holds for both clusters containing only one reflector and clusters containing multiple unresolved reflectors. Consequently, to model the object-generated measurements given a cluster hypothesis, we need to describe: 1) the probability of detecting a cluster, and 2) the distribution of that possible detection. The model of the individual reflector positions in the observation space and the model of their received signal amplitudes are discussed in Section IV-A. Based on these models, both the distribution of the object-generated detections and the probability of detecting a cluster is presented for a given cluster hypothesis in Section IV-B. Finally, how to generate the possible cluster hypotheses, \mathcal{C}_k , and evaluate their probabilities, $\Pr\{\mathcal{C}_k | \mathbf{x}_k\}$, is given in Section IV-C.

A. Reflector model

The full mathematical details of the reflector model (9) are given in Appendix A and summarised here for clarity. The purpose of the model, defined as

$$[(\mathbf{r}_k)^T, (\boldsymbol{\sigma}_k)^T]^T = h_\xi(\mathbf{x}_k) \quad (28)$$

is twofold: to, given \mathbf{x}_k , describe the position of the reflection centres in measurement space, \mathbf{r}_k , and to model the expected return signal amplitude from each centre, described by the parameter vector $\boldsymbol{\sigma}_k$. In our case, $\boldsymbol{\sigma}_k$ is a vector of Rayleigh parameters as we assume that the return signal power of reflector i , denoted A_k^i , is behaving according to the Swerling I model [22]. The Swerling I model stipulates that the amplitude of the received signal fluctuates between scans according to the Rayleigh distribution

$$A_k^i \sim \text{Rayleigh}(\sigma_k^i), \quad (29)$$

$$\text{where } \mathbb{E}\{A_k^i\} = \sigma_k^i \sqrt{\pi/2}.$$

B. Cluster model

We assume that the j^{th} measurement in \mathbf{y}_k^t originated from the i^{th} cluster in the cluster formation indicated by \mathcal{C}_k . This cluster is assumed to consist of a number of unresolved

reflectors⁴, and is defined by a set of reflector indices,

$$\mathcal{I}_i^C = \{l: \text{reflector number } l \text{ is in cluster number } i\}. \quad (30)$$

A simple, yet useful, model is to describe the (state dependent) signal component of a merged detection from this cluster as a weighted sum of the included reflection centres,

$$\mathbf{c}_k^{C,i} = \sum_{l \in \mathcal{I}_i^C} w_k^l \mathbf{r}_k^l, \quad (31)$$

where the weights are determined by the relative signal strength of the reflection centres according to

$$w_k^l = \frac{A_k^l}{\sum_{m \in \mathcal{I}_i^C} A_k^m}. \quad (32)$$

The signal amplitude of the cluster detection, denoted $A_k^{C,i}$, is also Rayleigh distributed but with parameter

$$\sigma_k^{C,i} = \sqrt{\left(\sum_{l \in \mathcal{I}_i^C} (\sigma_k^l)^2 \right)}. \quad (33)$$

Assuming additive Gaussian measurement noise, the j^{th} measurement in \mathbf{y}_k is

$$\mathbf{y}_k^{t,j} = \mathbf{c}_k^{C,i} + \mathbf{w}_k^j \quad (34)$$

where $\mathbf{w}_k^j \sim \mathcal{N}(\mathbf{0}, \mathbf{W}_k)$ denotes (sensor dependent) measurement noise, and the probability of receiving this detection is given by

$$P_{d,k}^{C,i} = \Pr \left\{ A_k^{C,i} > \gamma_A^s \mid \mathbf{x}_k \right\}. \quad (35)$$

Note that, even given \mathbf{x}_k , the signal component of the cluster measurement, $\mathbf{c}_k^{C,i}$, is stochastic as the weights w_k^j are stochastic. The distribution of $\mathbf{c}_k^{C,i}$ is defined by (29) – (32), which is difficult to evaluate. For this reason, we propose to approximate the cluster density as a Gaussian density, $p(\mathbf{c}_k^{C,i} \mid \mathbf{x}_k) \approx \mathcal{N}(\bar{\mathbf{c}}_k^{C,i}; \bar{\mathbf{c}}_k^{C,i}, \mathbf{C}_k^{C,i})$, with the same first two moments as the underlying distribution.

Let overscore denote the expected value of stochastic variables conditioned on \mathbf{x}_k , such that, e.g., $\bar{\mathbf{c}}_k^{C,i} = E \left\{ \mathbf{c}_k^{C,i} \mid \mathbf{x}_k \right\}$.

The first moment of \mathbf{c}_k^i , as given by (31), is

$$\bar{\mathbf{c}}_k^{C,i} = \sum_{l \in \mathcal{I}_i^C} \bar{w}_k^l \mathbf{r}_k^l \quad (36)$$

and after some manipulations, an expression for the covariance can be found as

$$\mathbf{C}_k^{C,i} = \sum_{s, t \in \mathcal{I}_i^C} \left(\mathbf{r}_k^s - \bar{\mathbf{c}}_k^{C,i} \right) \left(\mathbf{r}_k^t - \bar{\mathbf{c}}_k^{C,i} \right)^T \text{Cov} \{ w_k^s, w_k^t \}. \quad (37)$$

The position of each reflector, \mathbf{r}_k^i , is given by (100) in Appendix A, but we also need to express \bar{w}_k^i and $\text{Cov} \{ w_k^s, w_k^t \}$. As the moments of a Rayleigh distribution are well known, approximations of these quantities are readily found through Taylor expansion.

⁴A resolved reflector can be viewed as a cluster of reflectors where containing only one reflector.

C. Sensor resolution model

In [11], [19], a simple but qualitatively correct and tractable model is proposed for describing the probability that two point sources (targets) are unresolved by a radar sensor. Based on this two-source model, a sensor resolution model covering an arbitrary number of sources was derived in [20]. This model is also used in this paper to model the probability of receiving merged measurements from the reflection centres on the structure. We start by presenting the model in the case of two sources followed by the expansion to a more general formulation with multiple interacting sources.

1) *Two source model:* Denoting by \mathcal{U}_{ij} the event that reflector i and reflector j are positioned sufficiently close to be unresolved, a model for the probability of this pairwise cluster event is found in [11], [19] as,

$$\begin{aligned} \Pr \{ \mathcal{U}_{ij} \mid \mathbf{x}_k \} &= e^{-\frac{1}{2} (\Delta \mathbf{r}_k^{ij})^T (\mathbf{R}_u)^{-1} \Delta \mathbf{r}_k^{ij}} \\ &= |2\pi \mathbf{R}_u|^{1/2} \mathcal{N}(\mathbf{0}; \Delta \mathbf{r}_k^{ij}, \mathbf{R}_u), \end{aligned} \quad (38)$$

where $\Delta \mathbf{r}_k^{ij} = \mathbf{r}_k^i - \mathbf{r}_k^j$ is the distance between the reflectors in observation space and $\mathbf{R}_u = (2 \ln 2)^{-3/2} \text{diag} \{ [\delta_r, \delta_\phi, \delta_r]^2 \}$ represents the modelled resolution of the sensor. The parameters, δ_r , δ_ϕ and δ_r , describe the specified resolution capability of the sensor in each dimension of the observations space and are set based on sensor parameters such as the bandwidth, pulse duration and the antenna beam width. Note that the diagonal form of \mathbf{R}_u implies that the resolution capability of the sensor is modelled as independent in the different dimensions.

2) *Multi-source model:* The sensor resolution model for multiple sources in [20] is based on evaluating all possible pairwise interactions between the reflection sources. It is assumed that each reflector only has the possibility to independently interact with (to be pairwise connected to) its direct neighbours in each dimension of the observation space. In other words, projecting the position of the reflectors onto each dimension, a reflector can only interact with (connect to) the first reflector to the left and right in each dimension. The event that two neighbouring reflectors, i and j , are pairwise unresolved is modelled by the pairwise cluster event \mathcal{U}_{ij} and the probability of this event is assumed to be described by the two source resolution model in (38). Additionally, the cluster events for two different neighbours, \mathcal{U}_{ij} and \mathcal{U}_{ik} , are assumed mutually independent, and reflectors that are not direct neighbours are considered unresolved if they are connected through a series of pairwise cluster events.

The formulation of the resolution problem can be represented by a simple and undirected graph, here denoted \mathcal{G}_X , where the set of reflector indexes, $\mathcal{X} = \{1, 2, \dots, N_k^\xi\}$, are vertices and all possible pairwise cluster events, \mathcal{U}_{ij} , are edges. Thus, an edge between reflector i and j in \mathcal{G}_X describes the possibility for reflector i and j to be pairwise unresolved. Figure 3 shows two examples of the cluster hypothesis graph \mathcal{G}_X for three reflectors in two dimensions. In Figure 3a the reflectors are positioned on a straight line (as with our structure), whereas in Figure 3b, the reflectors are positioned in a triangular pattern. In Example B, all cluster events are possible between the three reflectors, but in Example A, the

cluster hypothesis graph has only two possible edges (cluster events), \mathcal{U}_{12} and \mathcal{U}_{23} . As the area spanned by reflector 1 and 3 encloses reflector 2 it is not possible that the cluster event \mathcal{U}_{13} is independent of \mathcal{U}_{12} and \mathcal{U}_{23} .

Let us again consider a cluster described by \mathcal{I}_i^C , as defined in (30). All possible pairwise cluster events (edges) between the reflectors in \mathcal{I}_i^C can be described by an *induced* subgraph⁵ to \mathcal{G}_X , denoted $\mathcal{G}_{\mathcal{I}_i^C}$. This induced subgraph has the vertices \mathcal{I}_i^C and the same edges between these vertices as in \mathcal{G}_X . In this context, a sufficient requirement for the reflectors in \mathcal{I}_i^C to be unresolved (form a joint detection) is that there exist at least one walk through $\mathcal{G}_{\mathcal{I}_i^C}$ including all reflectors (vertices). Generally there may exist multiple spanning subgraphs⁶ to $\mathcal{G}_{\mathcal{I}_i^C}$ for which this holds true. Returning to Example B in Figure 3b, if $\mathcal{I}_i^C = \{1, 2, 3\}$ (all reflectors are clustered), then any graph that contains at least two edges is a spanning subgraph. Let $\mathcal{S}_{\mathcal{I}_i^C}$ be the set of all unique spanning subgraphs for which there exists a walk including all reflectors in \mathcal{I}_i^C . Again, using the assumption that all possible cluster events are mutually independent, the probability that the reflectors in \mathcal{I}_i^C form a joint detection can be written as

$$\Pr \left\{ \mathcal{I}_i^C \text{ unresolved} \mid \mathbf{x}_k \right\} \triangleq P_c \{ \mathcal{I}_i^C \mid \mathbf{x}_k \} = \sum_{\mathcal{G}_j \in \mathcal{S}_{\mathcal{I}_i^C}} P_u \{ \mathcal{G}_j \mid \mathbf{x}_k \} P_r \{ \bar{\mathcal{G}}_j \mid \mathbf{x}_k \}, \quad (39)$$

where \mathcal{G}_j denotes one of the spanning subgraphs in $\mathcal{S}_{\mathcal{I}_i^C}$ and $\bar{\mathcal{G}}_j$ is its complement, i.e., if an edge exist in \mathcal{G}_j it is not in $\bar{\mathcal{G}}_j$ and vice versa. Further, $P_u \{ \cdot \mid \mathbf{x}_k \}$ and $P_r \{ \cdot \mid \mathbf{x}_k \}$ denote the probabilities that the reflectors connected by an edge in \mathcal{G} are unresolved or resolved, respectively, and are defined as

$$P_u \{ \mathcal{G} \mid \mathbf{x}_k \} \triangleq \prod_{u_{mn} \in \mathcal{G}} \Pr \{ \mathcal{U}_{mn} \mid \mathbf{x}_k \} \quad (40)$$

$$P_r \{ \mathcal{G} \mid \mathbf{x}_k \} \triangleq \prod_{u_{mn} \in \mathcal{G}} (1 - \Pr \{ \mathcal{U}_{mn} \mid \mathbf{x}_k \}), \quad (41)$$

For the example shown in Figure 3a, the probability that all reflectors are unresolved, i.e. $\mathcal{I}_i^C = \{1, 2, 3\}$, is

$$P_c \{ \mathcal{I}_i^C \mid \mathbf{x}_k \} = \Pr \{ \mathcal{U}_{12} \mid \mathbf{x}_k \} \Pr \{ \mathcal{U}_{23} \mid \mathbf{x}_k \}, \quad (42)$$

as there is only one walk, namely \mathcal{U}_{12} and \mathcal{U}_{23} , that connects all reflectors. For the example in Figure 3b, however, the same probability is formulated as

$$\begin{aligned} P_c \{ \mathcal{I}_i^C \mid \mathbf{x}_k \} &= \Pr \{ \mathcal{U}_{12} \mid \mathbf{x}_k \} \Pr \{ \mathcal{U}_{23} \mid \mathbf{x}_k \} (1 - \Pr \{ \mathcal{U}_{13} \mid \mathbf{x}_k \}) \\ &\quad + \Pr \{ \mathcal{U}_{12} \mid \mathbf{x}_k \} \Pr \{ \mathcal{U}_{13} \mid \mathbf{x}_k \} (1 - \Pr \{ \mathcal{U}_{23} \mid \mathbf{x}_k \}) \\ &\quad + \Pr \{ \mathcal{U}_{13} \mid \mathbf{x}_k \} \Pr \{ \mathcal{U}_{23} \mid \mathbf{x}_k \} (1 - \Pr \{ \mathcal{U}_{12} \mid \mathbf{x}_k \}) \\ &\quad + \Pr \{ \mathcal{U}_{12} \mid \mathbf{x}_k \} \Pr \{ \mathcal{U}_{13} \mid \mathbf{x}_k \} \Pr \{ \mathcal{U}_{23} \mid \mathbf{x}_k \}, \end{aligned} \quad (43)$$

as there exist four spanning subgraphs where there is one walk connecting all reflectors.

⁵An induced subgraph is a graph with a subset of the vertices of its parent but the same edges between these vertices.

⁶A spanning subgraph is a subgraph with the same vertices as its parent.

In the most general case, a cluster hypothesis \mathcal{C}_k indicates a set of disjoint cluster sets, $\mathcal{J}_k^C = \left\{ \mathcal{I}_i^C \right\}_{i=1}^{N_k^C}$, where we want to evaluate the probability that all reflectors are unresolved within each cluster and resolved between clusters. The probability of this cluster hypothesis can thus be written as

$$\begin{aligned} \Pr \{ \mathcal{C}_k \mid \mathbf{x}_k \} &= \left(\prod_{i=1}^{N_k^C} P_c \{ \mathcal{I}_i^C \mid \mathbf{x}_k \} \right) P_r \left\{ \mathcal{G}_X \setminus \bigcup_{u=1}^{N_k^C} \mathcal{G}_{\mathcal{I}_u^C} \mid \mathbf{x}_k \right\} \\ &= \left(\prod_{i=1}^{N_k^C} \sum_{\mathcal{G}_j \in \mathcal{S}_{\mathcal{I}_i^C}} P_u \{ \mathcal{G}_j \mid \mathbf{x}_k \} P_r \{ \bar{\mathcal{G}}_j \mid \mathbf{x}_k \} \right) \\ &\quad \times P_r \left\{ \mathcal{G}_X \setminus \bigcup_{u=1}^{N_k^C} \mathcal{G}_{\mathcal{I}_u^C} \mid \mathbf{x}_k \right\}. \end{aligned} \quad (44)$$

The first part in (44) describes the probability that the reflectors in each clusters are unresolved and the second part considers that all possible connections between different clusters, described by the graph $\mathcal{G}_X \setminus \bigcup_{u=1}^{N_k^C} \mathcal{G}_{\mathcal{I}_u^C}$, are resolved.

D. Summary

In this section we give a summary of the radar sensor model proposed in this paper. The clutter measurement vector, \mathbf{y}_k^c , can be found by generating the number of clutter measurements, m_k^c , according to (26), and then generate m_k^c independent clutter measurements in the manner of (27). To generate the target measurements, \mathbf{y}_k^t , the reflector positions in \mathbf{x}_k are mapped to the measurement space using (100). In order to probabilistically model the sensor's resolution capability we construct a set of cluster hypotheses, i.e. possible ways of partitioning the reflectors into inter-resolvable clusters, and evaluate their probabilities using (44). Under a cluster hypothesis, \mathcal{C}_k , there is a formation of N_k^C inter-resolvable clusters. Each of these clusters is detected with a probability, $P_{d,k}^{\mathcal{C},i}$, as described in (35), and the measurement generated by a detected cluster is given by (34). Conditioned on \mathcal{C}_k , the ordered object measurement vector can hence be described as

$$\begin{aligned} p(\mathbf{y}_k^t \mid \mathcal{C}_k, \mathbf{x}_k) &= \prod_{j=1}^{N_k^C} \left(1 - P_{d,k}^{\mathcal{C},j} \right) \times \sum_{1 \leq d_1 < \dots < d_{m_k^t} \leq N_k^C} \\ &\quad \prod_{j=1}^{m_k^t} \frac{P_{d,k}^{\mathcal{C},d_j}}{1 - P_{d,k}^{\mathcal{C},d_j}} \mathcal{N} \left(\mathbf{y}_k^t; \bar{\mathbf{c}}_k^{\mathcal{C},d_j}, \mathbf{C}_k^{\mathcal{C},d_j} + \mathbf{W}_k \right). \end{aligned} \quad (45)$$

This concludes the radar sensor model from which we can generate clutter as well as object-originated measurements, and where the limited resolution and detection capability of the sensor is taken into account.

V. POSTERIOR DENSITY

In this section we derive one recursion in the calculation of $p(\mathbf{x}_k \mid \mathbf{Y}_k)$. That is, we describe the update of the posterior from the previous scan, $p(\mathbf{x}_{k-1} \mid \mathbf{Y}_{k-1})$, with the new information in the observations made at time k . To accomplish

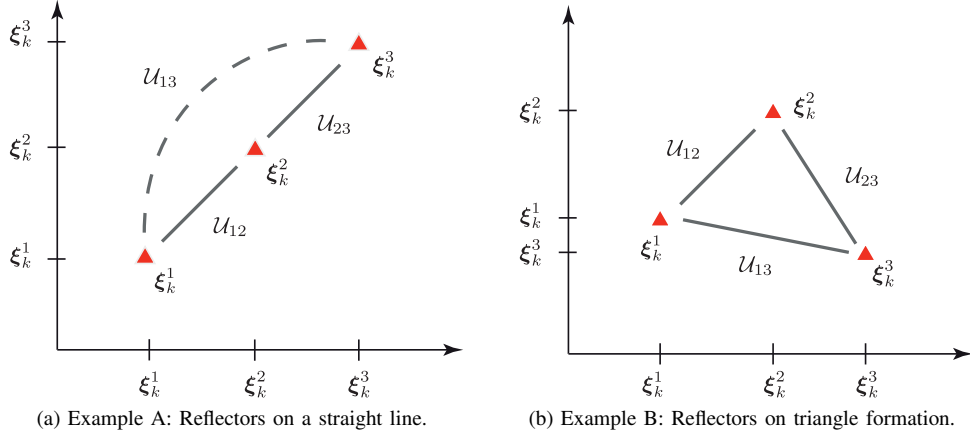


Figure 3. Example of two cluster hypothesis graphs containing three reflectors and two and three pairwise cluster events respectively.

this, we need to define the density from which the derivation starts. Furthermore, as mentioned in Section II-C, there are three types of uncertainties that need to be considered. There is uncertainty in the number of reflectors on the structure, in which reflectors that are resolved and which that are clustered, as well as in the association between the measurements in \mathbf{y}_k and the reflector clusters.

We start by introducing the posterior from the previous scan, followed by the introduction of a hypothesis set to handle the three types of uncertainties discussed above. Last but not least we derive an expression for the exact posterior density.

A. Posterior from the previous scan

We assume that the information in the observations up to and including time $k - 1$ indicate that a maximum number of N_{k-1}^ξ reflector centres exist on the structure. The existence variable, $e_{k-1}^i \in \{0, 1\}$ indicates whether the i^{th} reflector exist or not and we let $P_{e,k-1}^i = \Pr\{e_{k-1}^i = 1 | \mathbf{Y}_{k-1}\}$ denote the probability of existence of reflector i at time $k - 1$. Using this description, the density is assumed to be formulated (approximated) as,

$$p(\mathbf{x}_{k-1} | \mathbf{Y}_{k-1}) = \prod_{j=1}^{N_{k-1}^\xi} \left(1 - P_{e,k-1}^j\right) \times \sum_{\mathcal{E}_{k-1}} \left(\prod_{j=1}^{n_{k-1}^\xi} \frac{P_{e,k-1}^{i_j}}{1 - P_{e,k-1}^{i_j}} \right) \mathcal{N}(\mathbf{x}_{k-1}; \hat{\mathbf{x}}_{k-1}^{\mathcal{E}}, \mathbf{P}_{k-1}^{\mathcal{E}}). \quad (46)$$

where n_{k-1}^ξ is the number of reflectors in \mathbf{x}_{k-1} and \mathcal{E}_{k-1} is an existence hypothesis specifying an ordered set of existing reflector indices, $\{i_1, \dots, i_{n_{k-1}^\xi}\} = \{i : e_{k-1}^i = 1\}$, such that $1 \leq i_1 < \dots < i_{n_{k-1}^\xi} \leq N_{k-1}^\xi$. The vector $\hat{\mathbf{x}}_{k-1}^{\mathcal{E}}$ and the matrix $\mathbf{P}_{k-1}^{\mathcal{E}}$ are defined as

$$\hat{\mathbf{x}}_{k-1}^{\mathcal{E}} = \mathbb{E}\{\mathbf{x}_{k-1} | \mathcal{E}_{k-1}, \mathbf{Y}_{k-1}\} \quad (47)$$

$$\mathbf{P}_{k-1}^{\mathcal{E}} = \text{Cov}\{\mathbf{x}_{k-1} | \mathcal{E}_{k-1}, \mathbf{Y}_{k-1}\} \quad (48)$$

Note that the covariance matrix $\mathbf{P}_{k-1}^{\mathcal{E}}$ may include non-zero off-diagonal elements as the structure and feature states are correlated conditioned on data.

B. Hypothesis set

To compute $p(\mathbf{x}_k | \mathbf{Y}_k)$ from $p(\mathbf{x}_{k-1} | \mathbf{Y}_{k-1})$ we need to handle what we call *existence*, *cluster* and *data association* uncertainties. To facilitate this we introduce a coupled hypothesis set

$$\mathcal{H}_k = \{\mathcal{E}_k, \mathcal{C}_k, \mathcal{D}_k\} \quad (49)$$

where \mathcal{E}_k indicates the existence of one possible combination of reflector components, \mathcal{C}_k indicates one possible inter-resolvable cluster formation out of the existing reflectors and \mathcal{D}_k indicates one possible association between the clusters stipulated by \mathcal{C}_k and the measurements in \mathbf{y}_k . The set is coupled in the sense that an existence hypothesis generates a set of cluster hypotheses which, in turn, results in a set of possible measurement-to-cluster associations. More formal definitions of the different hypotheses are given below.

1) *Existence hypotheses*: Given that $\mathbf{x}_k | \mathbf{Y}_{k-1}$ can be described using a maximum of $N_k^\xi = N_{k-1}^\xi + N_k^b$ reflectors, we can define an existence hypothesis $\mathcal{E}_k = \{\mathcal{E}_k^s, \mathcal{E}_k^b\}$ indicating which of these reflectors actually exist at time k . The first part, \mathcal{E}_k^s , indicates which of the N_{k-1}^ξ possible reflectors existed at time $k-1$ and survived, whereas the second part, \mathcal{E}_k^b , indicates which of N_k^b possible new reflectors that are born.

2) *Cluster hypotheses*: The cluster hypotheses are thoroughly discussed in Section IV-C and summarised here for clarity. A cluster hypothesis \mathcal{C}_k stipulates one possible way of forming inter-resolvable cluster formations out of the reflectors given by the existence hypothesis, \mathcal{E}_k . Each \mathcal{C}_k describes a set of N_k^C disjoint reflector sets as

$$\mathcal{I}_k^C = \{\mathcal{I}_1^C, \mathcal{I}_2^C, \dots, \mathcal{I}_{N_k^C}^C\}, \quad (50)$$

where $\mathcal{I}_i^C = \{i_j\}_{j=1}^{N_i^C}$ such that $i_j \neq i_l$ if $j \neq l$ and if $m \in \mathcal{I}_i^C$ then $m \notin \mathcal{I}_j^C$.

3) *Data association hypotheses*: Given an existence hypothesis and a cluster hypothesis, there are still uncertainties regarding which of the clusters that are detected and the order of the measurement vector modelled by the permutation matrix $\Pi_p^{M_k}$ in (8). These uncertainties are treated with a data association hypothesis, \mathcal{D}_k , which indicates one possible association between the clusters, given by a cluster hypothesis

\mathcal{C}_k , and the M_k measurements in \mathbf{y}_k . Each data association hypothesis is connected to a data association vector,

$$\mathbf{d}_k = [d_1, d_2, \dots, d_{M_k}], \quad (51)$$

where $d_j = 0$ implies that \mathbf{y}_k^j originated from clutter and $d_j > 0$ implies that \mathbf{y}_k^j originated from cluster number d_j . Recall that the information regarding which reflectors that belong to cluster d_j is given by the cluster hypothesis \mathcal{C}_k .

C. Derivation of posterior density

From the previous posterior defined in Section V-A and using the hypothesis set introduced in Section V-B we want to derive a manageable expression for $p(\mathbf{x}_k | \mathbf{Y}_k)$. By marginalising over the hypothesis set, using Bayes' rule and the Markov property, the posterior density can be found as

$$\begin{aligned} p(\mathbf{x}_k | \mathbf{Y}_k) &= \sum_{\mathcal{H}_k} p(\mathbf{x}_k | \mathcal{H}_k, \mathbf{Y}_k) \Pr\{\mathcal{H}_k | \mathbf{Y}_k\} \\ &= \sum_{\mathcal{H}_k} \frac{p(\mathbf{y}_k | \mathcal{H}_k, \mathbf{x}_k, \mathbf{Y}_{k-1}) p(\mathbf{x}_k | \mathcal{H}_k, \mathbf{Y}_{k-1})}{p(\mathbf{y}_k | \mathcal{H}_k, \mathbf{Y}_{k-1})} \\ &\quad \times \frac{p(\mathbf{y}_k | \mathcal{H}_k, \mathbf{Y}_{k-1}) \Pr\{\mathcal{H}_k | \mathbf{Y}_{k-1}\}}{p(\mathbf{y}_k | \mathbf{Y}_{k-1})} \\ &= \sum_{\mathcal{H}_k} \frac{p(\mathbf{y}_k | \mathcal{H}_k, \mathbf{x}_k) \Pr\{\mathcal{C}_k, \mathcal{D}_k | \mathcal{E}_k, \mathbf{x}_k\} p(\mathbf{x}_k | \mathcal{E}_k, \mathbf{Y}_{k-1})}{p(\mathbf{y}_k | \mathbf{Y}_{k-1}) \Pr\{\mathcal{C}_k, \mathcal{D}_k | \mathcal{E}_k, \mathbf{Y}_{k-1}\}} \\ &\quad \times \Pr\{\mathcal{C}_k, \mathcal{D}_k | \mathcal{E}_k, \mathbf{Y}_{k-1}\} \Pr\{\mathcal{E}_k | \mathbf{Y}_{k-1}\} \\ &= \sum_{\mathcal{H}_k} \frac{p(\mathbf{y}_k | \mathcal{H}_k, \mathbf{x}_k) \Pr\{\mathcal{C}_k, \mathcal{D}_k | \mathcal{E}_k, \mathbf{x}_k\} p(\mathbf{x}_k | \mathcal{E}_k, \mathbf{Y}_{k-1})}{p(\mathbf{y}_k | \mathbf{Y}_{k-1})} \\ &\quad \times \Pr\{\mathcal{E}_k | \mathbf{Y}_{k-1}\}. \end{aligned} \quad (52)$$

Ignoring the proportionality constant, $p(\mathbf{y}_k | \mathbf{Y}_{k-1})$, and by splitting the sum over \mathcal{H}_k into the individual hypotheses, the sought posterior can be partitioned as

$$\begin{aligned} p(\mathbf{x}_k | \mathbf{Y}_k) &\propto \sum_{\mathcal{E}_k} \Pr\{\mathcal{E}_k | \mathbf{Y}_{k-1}\} \sum_{\mathcal{C}_k} \Pr\{\mathcal{C}_k | \mathcal{E}_k, \mathbf{x}_k\} \\ &\quad \times \sum_{\mathcal{D}_k} \Pr\{\mathcal{D}_k | \mathcal{C}_k, \mathcal{E}_k, \mathbf{x}_k\} p(\mathbf{y}_k | \mathcal{H}_k, \mathbf{x}_k) p(\mathbf{x}_k | \mathcal{E}_k, \mathbf{Y}_{k-1}). \end{aligned} \quad (53)$$

From (53), we see that the posterior can be partitioned into three mixtures, the sought posterior, and

$$\begin{aligned} p_{\mathcal{E}, \mathcal{C}}(\mathbf{x}_k | \mathbf{Y}_k) &= \\ \sum_{\mathcal{D}_k} \Pr\{\mathcal{D}_k | \mathcal{C}_k, \mathcal{E}_k, \mathbf{x}_k\} p(\mathbf{y}_k | \mathcal{H}_k, \mathbf{x}_k) p(\mathbf{x}_k | \mathcal{E}_k, \mathbf{Y}_{k-1}) \end{aligned} \quad (54)$$

$$p_{\mathcal{E}}(\mathbf{x}_k | \mathbf{Y}_k) = \sum_{\mathcal{C}_k} \Pr\{\mathcal{C}_k | \mathcal{E}_k, \mathbf{x}_k\} p_{\mathcal{E}, \mathcal{C}}(\mathbf{x}_k | \mathbf{Y}_k). \quad (55)$$

Each mixture considers one of the three uncertainties. Starting from the right in (53), an unnormalised mixture density, denoted $p_{\mathcal{E}, \mathcal{C}}(\mathbf{x}_k | \mathbf{Y}_k)$, is produced of posteriors for all data associations conditioned on an existence and a cluster hypothesis. Similarly, the mixture, $p_{\mathcal{E}}(\mathbf{x}_k | \mathbf{Y}_k)$, is created for all cluster formations under an existence hypothesis. Finally, the sought posterior is formulated as the mixture of $p_{\mathcal{E}}(\mathbf{x}_k | \mathbf{Y}_k)$ over all reflector existence hypotheses.

TABLE I
TRACKING FRAMEWORK ALGORITHM

1: Given $p(\mathbf{x}_{k-1}, \mathbf{Y}_{k-1})$
2: Construct existence hypotheses \mathcal{E}_k
3: For each \mathcal{E}_k
4: Calculate predicted density: $p(\mathbf{x}_k \mathcal{E}_k, \mathbf{Y}_{k-1}) \approx \mathcal{N}(\mathbf{x}_k; \hat{\mathbf{x}}_{k k-1}^{\mathcal{E}}, \mathbf{P}_{k k-1}^{\mathcal{E}})$
5: Construct cluster hypotheses \mathcal{C}_k
6: For each \mathcal{C}_k
7: Construct data association hypotheses \mathcal{D}_k
8: Measurement update (EKF or UKF): $q_{\mathcal{E}, \mathcal{C}, \mathcal{D}}(\mathbf{Y}_k) \mathcal{N}(\mathbf{x}_k; \hat{\mathbf{x}}_k^{\mathcal{H}}, \mathbf{P}_k^{\mathcal{H}})$ $\approx p(\mathbf{y}_k \mathcal{H}_k, \mathbf{x}_k) p(\mathbf{x}_k \mathcal{E}_k, \mathbf{Y}_{k-1})$
9: end
10: Form $p_{\mathcal{E}, \mathcal{C}}(\mathbf{x}_k \mathbf{Y}_k) =$ $\sum_{\mathcal{D}_k} \Pr\{\mathcal{D}_k \mathcal{C}_k, \mathcal{E}_k, \mathbf{Y}_{k-1}\} q_{\mathcal{E}, \mathcal{C}, \mathcal{D}}(\mathbf{Y}_k) \mathcal{N}(\mathbf{x}_k; \hat{\mathbf{x}}_k^{\mathcal{H}}, \mathbf{P}_k^{\mathcal{H}})$
11: Moment matching: $q_{\mathcal{E}, \mathcal{C}}(\mathbf{Y}_k) \mathcal{N}(\mathbf{x}_k; \hat{\mathbf{x}}_{k k}^{\mathcal{E}, \mathcal{C}}, \mathbf{P}_{k k}^{\mathcal{E}, \mathcal{C}}) \approx p_{\mathcal{E}, \mathcal{C}}(\mathbf{x}_k \mathbf{Y}_k)$
12: end
13: Resolution model update: $p_{\mathcal{E}}(\mathbf{x}_k \mathbf{Y}_k) \approx \sum_{\mathcal{C}_k} \beta_{\mathcal{C}}(\mathcal{E}, \mathbf{Y}_k) q_{\mathcal{E}, \mathcal{C}}(\mathbf{Y}_k) \mathcal{N}(\mathbf{x}_k; \hat{\mathbf{x}}_{k k}^{\mathcal{E}, \mathcal{C}}, \tilde{\mathbf{P}}_{k k}^{\mathcal{E}, \mathcal{C}})$
14: Moment matching: $q_{\mathcal{E}}(\mathbf{Y}_k) \mathcal{N}(\mathbf{x}_k; \hat{\mathbf{x}}_{k k}^{\mathcal{E}}, \mathbf{P}_{k k}^{\mathcal{E}}) \approx p_{\mathcal{E}}(\mathbf{x}_k \mathbf{Y}_k)$
15: end
16: Form posterior density: $p(\mathbf{x} \mathbf{Y}_k) \approx \frac{\Pr\{\mathcal{E}_k \mathbf{Y}_{k-1}\} q_{\mathcal{E}}(\mathbf{Y}_k) \mathcal{N}(\mathbf{x}_k; \hat{\mathbf{x}}_{k k}^{\mathcal{E}}, \mathbf{P}_{k k}^{\mathcal{E}})}{\sum_{\mathcal{E}_k} \Pr\{\mathcal{E}_k \mathbf{Y}_{k-1}\} q_{\mathcal{E}}(\mathbf{Y}_k)}$
17: Prune and merge

VI. TRACKING FRAMEWORK

In this section we propose a Bayesian tracking framework for calculating the posterior density derived in Section V, and an estimator for the extended object state. In order to arrive at a tractable solution we will find suitable approximations for each mixture density in (53) separately. Furthermore, we will propose methods for controlling the maximum number of possible reflection centres on the structure, N_k^{ξ} . This is important as the number of possible reflectors will influence the dimensionality of the hypothesis set \mathcal{H}_k and, consequently, also the number of components in the mixtures and the computational complexity.

The approach described here is a Kalman filter-like framework where each mixture is approximated by a Gaussian density with the same first two moments. Table I gives an overview of the different steps in the proposed framework and is intended as a guide throughout this section. A detailed discussion of the steps is given below, where the included densities are defined using the hypothesis set, \mathcal{H}_k , the structure and process models defined in Section III and the sensor model derived in Section IV.

A. Measurement update mixture

Given knowledge of which reflectors that exist on the structure (\mathcal{E}_k), and how they are partitioned into inter-resolvable clusters (\mathcal{C}_k), the tracking problem boils down to a non-linear point source multi-target tracking problem. The data association hypotheses specified by \mathcal{D}_k can be generated considering any suitable multi-target (point source) data association algorithm, such as JPDA [23] or GNN [1].

1) *Predicted density*: Conditioned on an existence hypothesis, the predicted density is given by (25) and (46) as

$$\begin{aligned} p(\mathbf{x}_k | \mathcal{E}_k, \mathbf{Y}_{k-1}) &= \int p(\mathbf{x}_k | \mathcal{E}_k, \mathbf{x}_{k-1}) p(\mathbf{x}_{k-1} | \mathcal{E}_k, \mathbf{Y}_{k-1}) d\mathbf{x}_{k-1} \\ &= \int \mathcal{N}(\mathbf{x}_k; \bar{\mathbf{x}}_k^{\mathcal{E}}, \mathbf{Q}_k^{\mathcal{E}}) \mathcal{N}(\mathbf{x}_{k-1}; \hat{\mathbf{x}}_{k-1}^{\mathcal{E}}, \mathbf{P}_{k-1}^{\mathcal{E}}) d\mathbf{x}_{k-1}. \end{aligned} \quad (56)$$

Like above, $\mathcal{E}_k = \{\mathcal{E}_k^s, \mathcal{E}_k^b\}$ states which reflectors that survive and which appear, and therefore (56) reduces to the problem of propagating a Gaussian density through a nonlinear function. A Gaussian approximation of this density is found as

$$p(\mathbf{x}_k | \mathcal{E}_k, \mathbf{Y}_{k-1}) \approx \mathcal{N}(\mathbf{x}_k; \hat{\mathbf{x}}_{k|k-1}^{\mathcal{E}}, \mathbf{P}_{k|k-1}^{\mathcal{E}}), \quad (57)$$

by propagating $\mathcal{N}(\mathbf{x}_{k-1}; \hat{\mathbf{x}}_{k-1}^{\mathcal{E}^s}, \mathbf{P}_{k-1}^{\mathcal{E}^s})$, given by (47) – (48), through the process model (24). In practice, the prediction is carried out in three steps. First, the structure state \mathbf{z}_{k-1} is propagated through the non-linear process model (14) using the unscented transform [24]. Second, the predicted positions of the surviving reflectors, stated in \mathcal{E}_k^s , are found using the survival process model (16) and the Kalman filter. Last, the predicted positions of the born reflectors in \mathcal{E}_k^b , are found through the birth process model (20).

2) *Measurement update*: Due to the assumption that the measurements are independent conditioned on \mathbf{x}_k and $\mathcal{H}_k = \{\mathcal{E}, \mathcal{C}, \mathcal{D}\}$, the likelihood function, $p(\mathbf{y}_k | \mathcal{H}_k, \mathbf{x}_k)$, can be decomposed as

$$p(\mathbf{y}_k | \mathcal{H}_k, \mathbf{x}_k) = \prod_{j=1}^{M_k} p(\mathbf{y}_k^j | \mathcal{H}_k, \mathbf{x}_k). \quad (58)$$

Conditioned on the current data association hypothesis, the measurement equation for the object generated measurements in (34) can be written as

$$\mathbf{y}_k^j = \mathbf{c}_k^{\mathcal{C}, d_j} + \mathbf{w}_k^j, \quad (59)$$

where $\mathbf{c}_k^{\mathcal{C}, d_j} | \mathbf{x}_k \sim \mathcal{N}(\bar{\mathbf{c}}_k^{\mathcal{C}, d_j}, \mathbf{C}_k^{\mathcal{C}, d_j})$ and $\mathbf{w}_k^j \sim \mathcal{N}(\mathbf{0}, \mathbf{W}_k)$. Note that $\bar{\mathbf{c}}_k^{\mathcal{C}, d_j}$ is a nonlinear function of the state according to (36). Using the measurement model in (59) and the clutter density in (27), each component in (58) is described by

$$p(\mathbf{y}_k^j | \mathcal{H}_k, \mathbf{x}_k) = \begin{cases} \mathcal{N}(\mathbf{y}_k^j; \bar{\mathbf{c}}_k^{\mathcal{C}, d_j}, \mathbf{C}_k^{\mathcal{C}, d_j} + \mathbf{W}_k) & \text{if } d_j \neq 0 \\ 1/V & \text{if } d_j = 0 \end{cases} \quad (60)$$

where V is the volume of the observation space.

The predicted density in (56) can now be updated using the likelihood in (58). From the Gaussian re-factorisation lemma [25], it is known that the product of two Gaussian densities describing two linearly dependent random vectors, e.g., \mathbf{x} and $\mathbf{y} = \mathbf{Hx} + \mathbf{n}$, where $\mathbf{n} \sim \mathcal{N}(\mathbf{0}, \mathbf{R})$, can be rewritten as

$$\mathcal{N}(\mathbf{y}; \mathbf{Hx}, \mathbf{R}) \mathcal{N}(\mathbf{x}; \hat{\mathbf{x}}_0, \mathbf{P}_0) = \mathcal{N}(\mathbf{y}; \hat{\mathbf{y}}, \mathbf{S}) \mathcal{N}(\mathbf{x}; \hat{\mathbf{x}}, \mathbf{P}). \quad (61)$$

As a function of \mathbf{x} , this is a scaled Gaussian density. The mean $\hat{\mathbf{y}}$ and the covariance \mathbf{S} are the first two moments of

$\mathbf{y} = \mathbf{Hx} + \mathbf{n}$, whereas $\hat{\mathbf{x}}$ and \mathbf{P} are given by the Kalman filter equations. To be able to apply this lemma on the product $p(\mathbf{y}_k | \mathcal{H}_k, \mathbf{x}_k) p(\mathbf{x}_k | \mathcal{E}_k, \mathbf{Y}_{k-1})$, where the mean of \mathbf{y}_k is a non-linear function of \mathbf{x}_k , we resort to a Gaussian approximation

$$\begin{aligned} p(\mathbf{y}_k | \mathcal{H}_k, \mathbf{x}_k) p(\mathbf{x}_k | \mathcal{E}_k, \mathbf{Y}_{k-1}) \\ \approx q_{\mathcal{E}, \mathcal{C}, \mathcal{D}}(\mathbf{Y}_k) \mathcal{N}(\mathbf{x}_k; \hat{\mathbf{x}}_{k|k}^{\mathcal{H}}, \mathbf{P}_{k|k}^{\mathcal{H}}). \end{aligned} \quad (62)$$

Here, $q_{\mathcal{E}, \mathcal{C}, \mathcal{D}}(\mathbf{Y}_k)$ is regarded as a scaling factor, and the density $\mathcal{N}(\mathbf{x}_k; \hat{\mathbf{x}}_{k|k}^{\mathcal{H}}, \mathbf{P}_{k|k}^{\mathcal{H}})$ is obtained from the update equations of the unscented Kalman filter (UKF) [24]. The scaling factor is found using the approximation

$$q_{\mathcal{E}, \mathcal{C}, \mathcal{D}}(\mathbf{Y}_k) \approx \left(\frac{1}{V}\right)^{M_k^c} \mathcal{N}(\mathbf{y}_k^{\text{t}, \mathcal{D}}; \hat{\mathbf{y}}_{k|k-1}^{\mathcal{H}}, \mathbf{P}_{\mathbf{yy}}^{\mathcal{H}}), \quad (63)$$

where M_k^c is the number of clutter measurements and $\mathbf{y}_k^{\text{t}, \mathcal{D}}$ is an ordered vector of the object measurements, under the current data association hypothesis. Approximations of the predicted measurement mean and covariance, $\hat{\mathbf{y}}_{k|k-1}^{\mathcal{H}}$ and $\mathbf{P}_{\mathbf{yy}}^{\mathcal{H}}$, are found as a part of the UKF update by propagating (56) through (59) using the unscented transform.

3) *Data association probability*: As stated in Section IV-A, the probability of detection, $P_{d,k}^i$, is assumed to be locally state independent. That is, $P_{d,k}^i$ is regarded as approximately constant where $\mathcal{N}(\mathbf{x}_k; \hat{\mathbf{x}}_{k|k}^{\mathcal{H}}, \mathbf{P}_{k|k}^{\mathcal{H}})$ has significant support, and thus, $\Pr\{\mathcal{D}_k | \mathcal{C}_k, \mathcal{E}_k, \mathbf{x}_k\} \approx \Pr\{\mathcal{D}_k | \mathcal{C}_k, \mathcal{E}_k, \mathbf{Y}_{k-1}\}$. This hypothesis probability, is calculated as

$$\begin{aligned} \Pr\{\mathcal{D}_k | \mathcal{C}_k, \mathcal{E}_k, \mathbf{Y}_{k-1}\} &= \Pr\{\mathbf{d}_k | \mathcal{C}_k, \mathcal{E}_k, \mathbf{Y}_{k-1}\} \\ &= \left(\frac{M_k^{\text{t}} + M_k^c}{M_k^{\text{t}}}\right)^{-1} \\ &\times \prod_{i=1}^{N_k^c} \left(1 - P_{d,k}^{\mathcal{C}, i}\right) \left(\prod_{d_j > 0} \frac{P_{d,k}^{C, d_j}}{1 - P_{d,k}^{C, d_j}}\right) \Pr\{M_k^c\}, \end{aligned} \quad (64)$$

where M_k^{t} and M_k^c are the number of object and clutter measurements, respectively. The probability $P_{d,k}^{\mathcal{C}, i}$ is found using $\mathbf{x}_k = \hat{\mathbf{x}}_{k-1}^{\mathcal{E}}$ in (35), and since M^c is Poisson distributed $\Pr\{M_k^c\} = (\mu V)^{M_k^c} \exp(-\mu V)/M_k^c!$.

4) *Moment matching*: Using (62) and (64) the measurement update mixture can be approximated as

$$\begin{aligned} p_{\mathcal{E}, \mathcal{C}}(\mathbf{x}_k | \mathbf{Y}_k) &\approx \\ \sum_{\mathcal{D}_k} \Pr\{\mathcal{D}_k | \mathcal{C}_k, \mathcal{E}_k, \mathbf{Y}_{k-1}\} q_{\mathcal{E}, \mathcal{C}, \mathcal{D}}(\mathbf{Y}_k) \mathcal{N}(\mathbf{x}_k; \hat{\mathbf{x}}_{k|k}^{\mathcal{H}}, \mathbf{P}_{k|k}^{\mathcal{H}}). \end{aligned} \quad (65)$$

In concurrence with the general idea of JPDA, this mixture is approximated as a single scaled Gaussian

$$p_{\mathcal{E}, \mathcal{C}}(\mathbf{x}_k | \mathbf{Y}_k) \approx q_{\mathcal{E}, \mathcal{C}}(\mathbf{Y}_k) \mathcal{N}(\mathbf{x}_k; \hat{\mathbf{x}}_{k|k}^{\mathcal{E}, \mathcal{C}}, \mathbf{P}_{k|k}^{\mathcal{E}, \mathcal{C}}), \quad (66)$$

using moment matching. The new scaling factor

$$q_{\mathcal{E}, \mathcal{C}}(\mathbf{Y}_k) = \sum_{\mathcal{D}_k} \Pr\{\mathcal{D}_k | \mathcal{C}_k, \mathcal{E}_k, \mathbf{Y}_{k-1}\} q_{\mathcal{E}, \mathcal{C}, \mathcal{D}}(\mathbf{Y}_k), \quad (67)$$

ensures that the integral $\int p_{\mathcal{E}, \mathcal{C}}(\mathbf{x}_k | \mathbf{Y}_k) d\mathbf{x}_k$ is identical in (65) and (66).

B. Resolution model mixture

In this section we discuss the resolution model mixture which, in (53), is defined as

$$p_{\mathcal{E}}(\mathbf{x}_k | \mathbf{Y}_k) = \sum_{\mathcal{C}_k} \Pr\{\mathcal{C}_k | \mathcal{E}_k, \mathbf{x}_k\} p_{\mathcal{E},\mathcal{C}}(\mathbf{x}_k | \mathbf{Y}_k). \quad (68)$$

In (66) the measurement update mixture is approximated as $p_{\mathcal{E},\mathcal{C}}(\mathbf{x}_k | \mathbf{Y}_k) \approx q_{\mathcal{E},\mathcal{C}}(\mathbf{Y}_k) \mathcal{N}(\mathbf{x}_k; \hat{\mathbf{x}}_{k|k}^{\mathcal{E},\mathcal{C}}, \mathbf{P}_{k|k}^{\mathcal{E},\mathcal{C}})$, where the density $\mathcal{N}(\mathbf{x}_k; \hat{\mathbf{x}}_{k|k}^{\mathcal{E},\mathcal{C}}, \mathbf{P}_{k|k}^{\mathcal{E},\mathcal{C}})$ will be affected by the resolution model, $\Pr\{\mathcal{C}_k | \mathcal{E}_k, \mathbf{x}_k\}$. In contrast to $\Pr\{\mathcal{D}_k | \mathcal{C}_k, \mathbf{x}_k\}$, the cluster hypothesis probability is not approximately locally constant. In fact, the resolution probability is strongly dependent on the relative distance between the reflectors in the measurement space (cf. (38)). As a result, $\Pr\{\mathcal{C}_k | \mathcal{E}_k, \mathbf{x}_k\}$ will not only influence the scaling of $p_{\mathcal{E},\mathcal{C}}(\mathbf{x}_k | \mathbf{Y}_k)$, but it will also contain information regarding the state and thus actually have effect on the shape of $p_{\mathcal{E}}(\mathbf{x}_k | \mathbf{Y}_k)$ as a function of \mathbf{x}_k .

In [19] it is shown how $\Pr\{\mathcal{C}_k | \mathcal{E}_k, \mathbf{x}_k\}$ influences a Gaussian density in the case of maximum two sources, which is extended to the case of an arbitrary but known number of sources in [20]. The principle derived in [20] is used also in this paper. We illustrate it for a simple two source example in Section VI-B1, and later generalise it to the case of multiple sources in Section VI-B2. For a more detailed description we refer the reader to [20].

1) Two source example: Suppose the existence hypothesis, \mathcal{E}_k , states that there exist two reflection centres on the structure, here called reflector i and j . Consequently, we have two possible cluster hypotheses; the reflectors are either resolved or clustered. Let us denote these cluster hypotheses as $\mathcal{C}_k = 1$ and $\mathcal{C}_k = 2$, respectively. Note that $\Pr\{\mathcal{C}_k | \mathcal{E}_k, \mathbf{x}_k\} = \Pr\{\mathcal{C}_k | \mathbf{x}_k\}$ since if \mathbf{x}_k is known, there are no uncertainties regarding the existence. This allow us to state the cluster hypothesis probabilities according to (44) as

$$\Pr\{\mathcal{C}_k = 1 | \mathcal{E}_k, \mathbf{x}_k\} = 1 - \Pr\{\mathcal{U}_{ij} | \mathcal{E}_k, \mathbf{x}_k\} \quad (69)$$

$$\Pr\{\mathcal{C}_k = 2 | \mathcal{E}_k, \mathbf{x}_k\} = \Pr\{\mathcal{U}_{ij} | \mathcal{E}_k, \mathbf{x}_k\}, \quad (70)$$

where

$$\Pr\{\mathcal{U}_{ij} | \mathcal{E}_k, \mathbf{x}_k\} = |2\pi\mathbf{R}_u|^{1/2} \mathcal{N}\left(\mathbf{0}; \Delta\mathbf{r}_k^{ij}, \mathbf{R}_u\right), \quad (71)$$

as given by (38).

Additionally, assuming that the object state after measurement update under each of the two cluster hypotheses can be described by the Gaussian densities $\mathcal{N}(\mathbf{x}_k; \hat{\mathbf{x}}_{k|k}^{\mathcal{E},1}, \mathbf{P}_{k|k}^{\mathcal{E},1})$ and $\mathcal{N}(\mathbf{x}_k; \hat{\mathbf{x}}_{k|k}^{\mathcal{E},2}, \mathbf{P}_{k|k}^{\mathcal{E},2})$, respectively, the resolution mixture components are

$$\begin{aligned} & \Pr\{\mathcal{C}_k = 1 | \mathcal{E}_k, \mathbf{x}_k\} \mathcal{N}\left(\mathbf{x}_k; \hat{\mathbf{x}}_{k|k}^{\mathcal{E},1}, \mathbf{P}_{k|k}^{\mathcal{E},1}\right) \\ &= (1 - \Pr\{\mathcal{U}_{ij} | \mathcal{E}_k, \mathbf{x}_k\}) \mathcal{N}\left(\mathbf{x}_k; \hat{\mathbf{x}}_{k|k}^{\mathcal{E},1}, \mathbf{P}_{k|k}^{\mathcal{E},1}\right) \\ &= \mathcal{N}\left(\mathbf{x}_k; \hat{\mathbf{x}}_{k|k}^{\mathcal{E},1}, \mathbf{P}_{k|k}^{\mathcal{E},1}\right) - \\ &= |2\pi\mathbf{R}_u|^{1/2} \mathcal{N}\left(\mathbf{0}; \Delta\mathbf{r}_k^{ij}, \mathbf{R}_u\right) \mathcal{N}\left(\mathbf{x}_k; \hat{\mathbf{x}}_{k|k}^{\mathcal{E},1}, \mathbf{P}_{k|k}^{\mathcal{E},1}\right) \quad (72) \\ & \Pr\{\mathcal{C}_k = 2 | \mathcal{E}_k, \mathbf{x}_k\} \mathcal{N}\left(\mathbf{x}_k; \hat{\mathbf{x}}_{k|k}^{\mathcal{E},2}, \mathbf{P}_{k|k}^{\mathcal{E},2}\right) \end{aligned}$$

$$\begin{aligned} &= \Pr\{\mathcal{U}_{ij} | \mathcal{E}_k, \mathbf{x}_k\} \mathcal{N}\left(\mathbf{x}_k; \hat{\mathbf{x}}_{k|k}^{\mathcal{E},2}, \mathbf{P}_{k|k}^{\mathcal{E},2}\right) \\ &= |2\pi\mathbf{R}_u|^{1/2} \mathcal{N}\left(\mathbf{0}; \Delta\mathbf{r}_k^{ij}, \mathbf{R}_u\right) \mathcal{N}\left(\mathbf{x}_k; \hat{\mathbf{x}}_{k|k}^{\mathcal{E},2}, \mathbf{P}_{k|k}^{\mathcal{E},2}\right). \quad (73) \end{aligned}$$

In this context, the factors $\mathcal{N}\left(\mathbf{0}; \Delta\mathbf{r}_k^{ij}, \mathbf{R}_u\right)$ can be considered as describing a non-linear pseudo-measurement model, with additive Gaussian noise

$$\delta_k^{ij} = \Delta\mathbf{r}_k^{ij} + \mathbf{w}_k^u = \mathbf{r}_k^i - \mathbf{r}_k^j + \mathbf{w}_k^u \quad (74)$$

where \mathbf{r}_k^j and \mathbf{r}_k^i are non-linear functions of \mathbf{x}_k as described in (100), and $\mathbf{w}_k^u \sim \mathcal{N}(\mathbf{0}, \mathbf{R}_u)$. The received pseudo-measurement of the relative distance between the reflectors is always $\delta_k^{ij} = \mathbf{0}$. As a result, the product

$\mathcal{N}\left(\mathbf{0}; \Delta\mathbf{r}_k^{ij}, \mathbf{R}_u\right) \mathcal{N}\left(\mathbf{x}_k; \hat{\mathbf{x}}_{k|k}^{\mathcal{E},2}, \mathbf{P}_{k|k}^{\mathcal{E},2}\right)$ can be considered as a measurement update step using the non-linear measurement equation (74) and the measurement $\delta_k^{ij} = \mathbf{0}$. Again using the approximation of the Gaussian re-factorisation lemma, a Gaussian approximation of this measurement update is found using the UKF update equations as

$$\begin{aligned} & |2\pi\mathbf{R}_u|^{1/2} \mathcal{N}\left(\mathbf{0}; \Delta\mathbf{r}_k^{ij}, \mathbf{R}_u\right) \mathcal{N}\left(\mathbf{x}_k; \hat{\mathbf{x}}_{k|k}^{\mathcal{E},2}, \mathbf{P}_{k|k}^{\mathcal{E},2}\right) \\ & \approx |2\pi\mathbf{R}_u|^{1/2} \mathcal{N}\left(\mathbf{0}; \hat{\delta}_k^{ij}, \mathbf{P}_{\delta\delta}^{ij}\right) \mathcal{N}\left(\mathbf{x}_k; \hat{\mathbf{x}}_{k|k}^{\mathcal{E},2,\mathcal{U}_{ij}}, \mathbf{P}_{k|k}^{\mathcal{E},2,\mathcal{U}_{ij}}\right) \quad (75) \end{aligned}$$

where $\hat{\delta}_k^{ij}$ the predicted relative distance between the reflectors and $\mathbf{P}_{\delta\delta}^{ij}$ is the corresponding covariance conditioned on \mathbf{Y}_k . We approximate these using the unscented transform and the “pseudo-measurement equation” in (74). The updated mean $\hat{\mathbf{x}}_{k|k}^{\mathcal{E},2,\mathcal{U}_{ij}}$ and covariance $\mathbf{P}_{k|k}^{\mathcal{E},2,\mathcal{U}_{ij}}$ are found using the corresponding Kalman filter update equations with $\delta_k^{ij} = \mathbf{0}$ as observation. Denoting

$$\beta_{\mathcal{U}_{ij}}(\mathcal{E}_k, \mathbf{Y}_k) = |2\pi\mathbf{R}_u|^{1/2} \mathcal{N}\left(\mathbf{0}; \hat{\delta}_k^{ij}, \mathbf{P}_{\delta\delta}^{ij}\right), \quad (76)$$

the expressions in (72) and (73) can be written as

$$\begin{aligned} & \Pr\{\mathcal{C}_k = 1 | \mathcal{E}_k, \mathbf{x}_k\} \mathcal{N}\left(\mathbf{x}_k; \hat{\mathbf{x}}_{k|k}^{\mathcal{E},1}, \mathbf{P}_{k|k}^{\mathcal{E},1}\right) \\ & \approx \mathcal{N}\left(\mathbf{x}_k; \hat{\mathbf{x}}_{k|k}^{\mathcal{E},1}, \mathbf{P}_{k|k}^{\mathcal{E},1}\right) - \\ & \Pr_{\mathcal{U}_{ij}}(\mathcal{E}_k, \mathbf{Y}_k) \mathcal{N}\left(\mathbf{x}_k; \hat{\mathbf{x}}_{k|k}^{\mathcal{E},1,\mathcal{U}_{ij}}, \mathbf{P}_{k|k}^{\mathcal{E},1,\mathcal{U}_{ij}}\right) \quad (77) \end{aligned}$$

$$\begin{aligned} & \Pr\{\mathcal{C}_k = 2 | \mathcal{E}_k, \mathbf{x}_k\} \mathcal{N}\left(\mathbf{x}_k; \hat{\mathbf{x}}_{k|k}^{\mathcal{E},2}, \mathbf{P}_{k|k}^{\mathcal{E},2}\right) \approx \\ & \Pr_{\mathcal{U}_{ij}}(\mathcal{E}_k, \mathbf{Y}_k) \mathcal{N}\left(\mathbf{x}_k; \hat{\mathbf{x}}_{k|k}^{\mathcal{E},2,\mathcal{U}_{ij}}, \mathbf{P}_{k|k}^{\mathcal{E},2,\mathcal{U}_{ij}}\right). \quad (78) \end{aligned}$$

By again approximating the updated mixture densities for each cluster hypothesis as a scaled Gaussian density, $\beta_{\mathcal{C}}(\mathcal{E}_k, \mathbf{Y}_k) \mathcal{N}\left(\mathbf{x}_k; \tilde{\mathbf{x}}_{k|k}^{\mathcal{E},\mathcal{C}}, \tilde{\mathbf{P}}_{k|k}^{\mathcal{E},\mathcal{C}}\right)$, the resulting resolution model mixture can be written as

$$\begin{aligned} & p_{\mathcal{E}}(\mathbf{x}_k | \mathbf{Y}_k) \\ & \approx \sum_{\mathcal{C}_k} q_{\mathcal{E},\mathcal{C}}(\mathbf{Y}_k) \beta_{\mathcal{C}}(\mathcal{E}_k, \mathbf{Y}_k) \mathcal{N}\left(\mathbf{x}_k; \tilde{\mathbf{x}}_{k|k}^{\mathcal{E},\mathcal{C}}, \tilde{\mathbf{P}}_{k|k}^{\mathcal{E},\mathcal{C}}\right). \quad (79) \end{aligned}$$

Here, $\tilde{\mathbf{x}}_{k|k}^{\mathcal{E},\mathcal{C}}$ and $\tilde{\mathbf{P}}_{k|k}^{\mathcal{E},\mathcal{C}}$ denote the first and second moment of the updated mixture density, whereas $\beta_{\mathcal{C}}(\mathcal{E}_k, \mathbf{Y}_k)$ is selected

to ensure that $\int \Pr\{\mathcal{C}_k | \mathcal{E}_k, \mathbf{x}_k\} \mathcal{N}\left(\mathbf{x}_k; \hat{\mathbf{x}}_{k|k}^{\mathcal{E}, \mathcal{C}}, \mathbf{P}_{k|k}^{\mathcal{E}, \mathcal{C}}\right) d\mathbf{x}_k = \int \beta_{\mathcal{C}}(\mathcal{E}_k, \mathbf{Y}_k) \mathcal{N}\left(\mathbf{x}_k; \tilde{\mathbf{x}}_{k|k}^{\mathcal{E}, \mathcal{C}}, \tilde{\mathbf{P}}_{k|k}^{\mathcal{E}, \mathcal{C}}\right) d\mathbf{x}_k = \beta_{\mathcal{C}}(\mathcal{E}_k, \mathbf{Y}_k)$. For instance, in (77) we get $\beta_{\mathcal{C}}(\mathcal{E}_k, \mathbf{Y}_k) = 1 - \beta_{\mathcal{U}_{ij}}(\mathcal{E}_k, \mathbf{Y}_k)$.

2) *General example and further approximations:* In its most general form, the cluster hypothesis probability, as defined in (44), consists of a product of sums

$$\begin{aligned} \Pr\{\mathcal{C}_k | \mathcal{E}_k, \mathbf{x}_k\} &= \\ &\prod_{i=1}^{N_k^c} \left(\sum_{\mathcal{G}_j \in \mathcal{S}_{\mathcal{I}_i^c}} \Pr_{\mathbf{x}_k} \{\mathcal{G}_j | \mathbf{x}_k\} \Pr\{\bar{\mathcal{G}}_j | \mathbf{x}_k\} \right) \\ &\times \Pr \left\{ \mathcal{G}_{\xi} \setminus \bigcup_{u=1}^{N_k^c} \mathcal{G}_{\mathcal{I}_u^c} | \mathbf{x}_k \right\}. \end{aligned}$$

Through expansion, this expression can be transformed into a sum of products where each term can be considered independently. Each term in the sum will have the same form as the terms in (72) – (73), however, in the general case each term can be the product of several probabilities, $\Pr\{\mathcal{U}_{ij} | \mathbf{x}_k\}$, and a Gaussian density. We have seen how to treat the product of

$$\Pr\{\mathcal{U}_{ij} | \mathbf{x}_k\} \mathcal{N}\left(\mathbf{x}_k; \hat{\mathbf{x}}_{k|k}^{\mathcal{E}, \mathcal{C}}, \mathbf{P}_{k|k}^{\mathcal{E}, \mathcal{C}}\right),$$

in the case of two sources and in the general case this is done recursively to replace the full product by a scaled Gaussian density. The resulting sum of scaled Gaussian densities is then approximated by $\beta_{\mathcal{C}}(\mathcal{E}_k, \mathbf{Y}_k) \mathcal{N}\left(\mathbf{x}_k; \tilde{\mathbf{x}}_{k|k}^{\mathcal{E}, \mathcal{C}}, \tilde{\mathbf{P}}_{k|k}^{\mathcal{E}, \mathcal{C}}\right)$ in the same manner as for the case of two sources. The mixture $p_{\mathcal{E}}(\mathbf{x}_k | \mathbf{Y}_k)$ is found by considering all possible cluster hypotheses

$$\begin{aligned} p_{\mathcal{E}}(\mathbf{x}_k | \mathbf{Y}_k) &\approx \sum_{\mathcal{C}_k} q_{\mathcal{E}, \mathcal{C}}(\mathbf{Y}_k) \beta_{\mathcal{C}}(\mathcal{E}_k, \mathbf{Y}_k) \mathcal{N}\left(\mathbf{x}_k; \tilde{\mathbf{x}}_{k|k}^{\mathcal{E}, \mathcal{C}}, \tilde{\mathbf{P}}_{k|k}^{\mathcal{E}, \mathcal{C}}\right) \\ &\approx q_{\mathcal{E}}(\mathbf{Y}_k) \mathcal{N}\left(\mathbf{x}_k; \hat{\mathbf{x}}_{k|k}^{\mathcal{E}}, \mathbf{P}_{k|k}^{\mathcal{E}}\right), \end{aligned} \quad (80)$$

where $\hat{\mathbf{x}}_{k|k}^{\mathcal{E}}$ and $\mathbf{P}_{k|k}^{\mathcal{E}}$ are found as the first two moments of

$$\frac{\sum_{\mathcal{C}_k} q_{\mathcal{E}, \mathcal{C}}(\mathbf{Y}_k) \beta_{\mathcal{C}}(\mathcal{E}_k, \mathbf{Y}_k) \mathcal{N}\left(\mathbf{x}_k; \tilde{\mathbf{x}}_{k|k}^{\mathcal{E}, \mathcal{C}}, \tilde{\mathbf{P}}_{k|k}^{\mathcal{E}, \mathcal{C}}\right)}{q_{\mathcal{E}}(\mathbf{Y}_k)}, \quad (81)$$

and the scaling factor is

$$q_{\mathcal{E}}(\mathbf{Y}_k) = \sum_{\mathcal{C}_k} q_{\mathcal{E}, \mathcal{C}}(\mathbf{Y}_k) \beta_{\mathcal{C}}(\mathcal{E}_k, \mathbf{Y}_k). \quad (82)$$

C. Existence model mixture

The final expression of the posterior density is found using (80) as

$$\begin{aligned} p(\mathbf{x}_k | \mathbf{Y}_k) &\propto \sum_{\mathcal{E}_k} \Pr\{\mathcal{E}_k | \mathbf{Y}_{k-1}\} p_{\mathcal{E}}(\mathbf{x}_k | \mathbf{Y}_k) \\ &\approx \sum_{\mathcal{E}_k} \Pr\{\mathcal{E}_k | \mathbf{Y}_{k-1}\} q_{\mathcal{E}}(\mathbf{Y}_k) \mathcal{N}\left(\mathbf{x}_k; \hat{\mathbf{x}}_{k|k}^{\mathcal{E}}, \mathbf{P}_{k|k}^{\mathcal{E}}\right), \end{aligned} \quad (83)$$

where

$$\begin{aligned} \Pr\{\mathcal{E}_k | \mathbf{Y}_{k-1}\} &= \Pr\{\mathcal{E}_k^s | \mathbf{Y}_{k-1}\} \Pr\{\mathcal{E}_k^b | \mathbf{Y}_{k-1}\} \\ &= \prod_{i \notin \mathcal{E}_k^s} (1 - P_{s,k}^i P_{e,k-1}^i) \prod_{i \in \mathcal{E}_k^s} P_{s,k}^i P_{e,k-1}^i \\ &\times \prod_{i \notin \mathcal{E}_k^b} (1 - P_{b,k}^i) \prod_{i \in \mathcal{E}_k^b} P_{b,k}^i. \end{aligned} \quad (84)$$

The updated existence hypotheses are found as

$$\Pr\{\mathcal{E}_k | \mathbf{Y}_k\} = \frac{\Pr\{\mathcal{E}_k | \mathbf{Y}_{k-1}\} q_{\mathcal{E}}(\mathbf{Y}_k)}{\sum_{\mathcal{E}_k} \Pr\{\mathcal{E}_k | \mathbf{Y}_{k-1}\} q_{\mathcal{E}}(\mathbf{Y}_k)}. \quad (85)$$

Using (85), the probability of existence for a reflector i at time k can be calculated as

$$P_{e,k}^i = \sum_{\mathcal{E}_k^i} \Pr\{\mathcal{E}_k^i | \mathbf{Y}_k\}, \quad (86)$$

where \mathcal{E}_k^i are the existence hypotheses where reflector i exists. Using this expression, the posterior density can be written on the same form as the posterior from the previous time index from which we started,

$$\begin{aligned} p(\mathbf{x}_k | \mathbf{Y}_k) &= \\ &= \prod_{j=1}^{N_k^{\xi}} \left(1 - P_{e,k}^j \right) \sum_{\mathcal{E}_k} \left(\prod_{j=1}^{n_k^{\xi}} \frac{P_{e,k}^{i,j}}{1 - P_{e,k}^{i,j}} \right) \mathcal{N}\left(\mathbf{x}_k; \hat{\mathbf{x}}_k^{\mathcal{E}}, \mathbf{P}_k^{\mathcal{E}}\right). \end{aligned} \quad (87)$$

D. Merge and prune

To limit the number of possible reflectors on the structure to a tractable number, we propose to prune unlikely reflection centres, and to merge reflection centres that are closely spaced. The pruning of reflectors is performed by removing reflectors with a probability of existence lower than a pre-specified threshold γ_e .

Like the algorithm proposed in [26], the merging algorithm proposed here starts by choosing the most probable reflector, i.e., the reflector with the largest $P_{e,k}^i$, and then grouping the reflectors that are within some distance from this reflector. Subsequently, the most probable reflector out of the remaining reflectors is considered in the same manner. This is repeated until all reflectors are included in a group. Consequently, $N_k^g \leq N_k^{\xi}$ groups are constructed where the i^{th} group is formed as

$$\mathbf{g}_k^i = [g_1^i, \dots, g_{N_i}^i], \quad (88)$$

where g_j^i is the index of the j^{th} reflector in group i .

Each group of reflectors is replaced by one new reflection centre. The probability of existence for the new reflector is calculated using local existence hypotheses defining which reflectors within the group that exist. To indicate whether a reflector exists or not, we use an existence variable $e_{g,k}^{i,j} \in \{0, 1\}$, such that $e_{g,k}^{i,j} = 1$ indicates that reflector g_j^i exists and vice versa for $e_{g,k}^{i,j} = 0$. An existence hypothesis for group i can then be described by the vector $\mathbf{e}_{g,k}^i = [e_{g,k}^{i,1}, \dots, e_{g,k}^{i,N_i}]$, and the

probability of existence for the new reflector is

$$\begin{aligned} P_{g,k}^i &= \sum_{\mathbf{e}_{g,k}^i \neq \mathbf{0}} \Pr \{ \mathbf{e}_{g,k}^i | \mathbf{Y}_k \} \\ &= \sum_{\mathbf{e}_{g,k}^i \neq \mathbf{0}} \prod_{\{j: e_{g,k}^{i,j}=0\}} \left(1 - P_{e,k}^{g_j^i}\right) \prod_{\{j: e_{g,k}^{i,j}=1\}} P_{e,k}^{g_j^i}. \end{aligned} \quad (89)$$

The position of the group reflector is described as

$$l_k^{g,i} = \frac{1}{P_{g,k}^i} \sum_{\mathbf{e}_{g,k}^i \neq \mathbf{0}} \Pr \{ \mathbf{e}_{g,k}^i | \mathbf{Y}_k \} f_g^i(\xi_k, \mathbf{e}_{g,k}^i) \quad (90)$$

where $f_g^i(\cdot)$ models the position of the new reflector for a given existence hypothesis as,

$$f_g^i(\xi_k, \mathbf{e}_{g,k}^i) = \frac{1}{N_i} \sum_{\{j: e_{g,k}^{i,j}=1\}} l_k^j. \quad (91)$$

From the N_k^g groups of reflectors, the state vector representing the extended target can be stated as

$$\mathbf{x}_k^g = \left[\mathbf{z}_k^T, l_k^{g,1}, \dots, l_k^{g,N_k^g} \right]^T \sim \mathcal{N} \left(\hat{\mathbf{x}}_{k|k}^g, \mathbf{P}_{k|k}^g \right) \quad (92)$$

where

$$\hat{\mathbf{x}}_{k|k}^g = \mathbb{E} \{ \mathbf{x}_k^g | \mathbf{Y}_k \}, \quad \mathbf{P}_{k|k}^g = \text{Cov} \{ \mathbf{x}_k^g | \mathbf{Y}_k \}. \quad (93)$$

The full description of the extended target given measurements up to time k , is found using (89), (92) and the model for the updated density in (87).

VII. EVALUATION

In this section, we evaluate the proposed models and the tracking framework on a vehicle scenario. The evaluation is performed using real radar data and we compare our proposed tracking framework to that presented in [3]. This comparison is performed both regarding estimation error in position, heading and speed of the vehicle, and regarding how well the vehicle extent is described.

A. The evaluation setting

This section describes the scenario and the radar data used for evaluation. The model to which we compare our proposed model will also be briefly discussed and last we give some details about the implementations.

1) Sensor types: For the evaluation, radar data is collected from three sensors mounted on a host vehicle as illustrated in Figure 4. The sensor denoted s_1 is a 77 GHz long-range radar with an update rate of 10 Hz, a field of view of 16° and a detection range of approximately 150 metres. The sensors s_2 and s_3 , are 24 GHz medium-range radars covering a 150° field of view up to approximately 70 metres using 13 independent receive beams, each delivering detections every 40 ms. The resolution cell for the sensor s_1 is described by the vector $[\delta_r, \delta_\phi, \delta_r]^{s_1} = [2m, 3.5^\circ, .5m/s]$, and for each receiving beam in s_2 and s_3 , the resolution is given by $[\delta_r, \delta_\phi, \delta_r]^{s_{2,3}} = [2m, \infty, 6m/s]$. The measurement noise covariance for a point target is specified as $\mathbf{W}_k^{s_1} = \text{diag} \{ [.4, \frac{1\pi}{180}, .5] \}^2$ and $\mathbf{W}_k^{s_{2,3}} = \text{diag} \{ [.4, \frac{1.2\pi}{180}, 2] \}^2$. The host and target reference positions are acquired using accurate DGPS data.

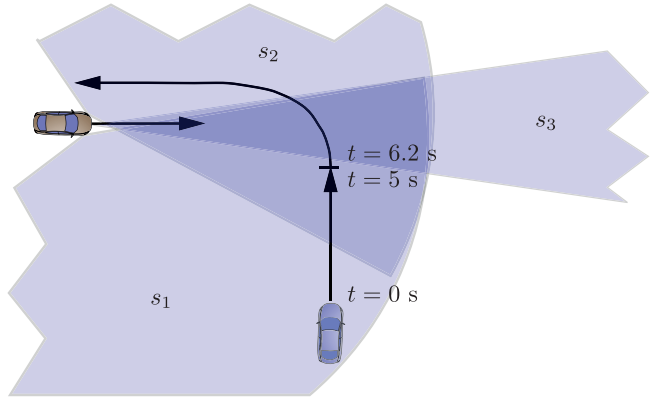


Figure 4. Host vehicle equipped with three radar sensors, one mechanically scanned 77 Ghz long range radar, denoted s_1 , and two medium range 24 GHz radars looking to the right and left, denoted s_2 and s_3 , respectively. In the evaluated tracking scenario the host vehicle is travelling at constant speed along a straight path. The target vehicle drives at a crossing path stopping in front of the host vehicle before making a left turn.

2) Tracking scenario: Data is collected in the scenario depicted in Figure 4, where the host is driving at a constant speed towards an intersection. The target vehicle approaches from the right, and makes a short stop before it turns left to meet the host. This scenario has been chosen since it is a challenging situation for tracking using radar measurements, as the target vehicle is travelling almost radially to the sensor which means that the observability of the full velocity vector is low.

3) The vehicle tracking framework used for comparison: As a reference we use the vehicle tracking framework in [3]. In this framework it is assumed that the positions of the reflection centres are deterministic, conditioned on the target vehicle state. Hence in contrast to our framework, there are no uncertainties regarding the dimension of the tracked vehicle, the number of reflection centres or their positions. The framework uses the same state representation as the structure state, \mathbf{z}_k , but without the angle θ_k , and the rotation point is fixed to the middle of the rear axle. Moreover, this framework incorporate a radar sensor model that considers the effects of limited resolution for a general number of reflection centres. Reflectors that are likely to be unresolved by the sensor form groups where each group is capable of generating multiple measurements. Included are models for the number of detections from a group as well as the distribution of the resulting detections.

4) Filter parameters: Both filters are initiated in the reference state, $[x_0, y_0, \psi_0, v_0, c_0, a_0]^T$, provided by the DGPS. In addition, our filter is initiated in the angle $\theta_0 = 0$ and with the feature state vector $\xi_0 = l_0^1 = 0$, i.e., the structure has only one reflector. The corresponding covariances are $\mathbf{P}_0 = \text{diag} \{ [1, 1, \frac{3\pi}{180}, .5, .001, 1.5, \frac{5\pi}{180}, .4] \}^2$ for our proposed model, and $\mathbf{P}_0 = \text{diag} \{ [1, 1, \frac{3\pi}{180}, .5, .001, 1.5] \}^2$ for the vehicle tracking model. The process noise used in the filters are acceleration noise, $\sigma_a^2 = 1.5^2$, curvature noise whose variance σ_c^2 depends on the velocity, and additional for our proposed framework, $\sigma_\theta^2 = (\frac{0.1\pi}{180})^2$ and $\sigma_l^2 = .05^2$. At each time k , the birth model allows a maximum of $B_k = 2$

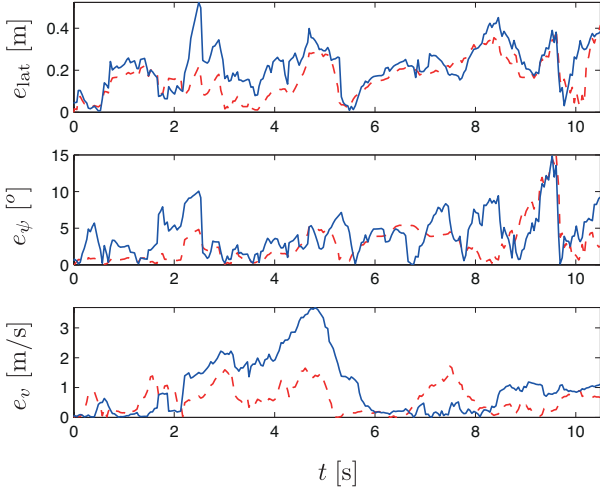


Figure 5. Error in estimated lateral position, e_{lat} , heading angle, e_ψ , and velocity, e_v . The solid (blue) lines shows the result for our proposed tracking framework and the dashed (red) lines for the vehicle tracking framework

new reflectors to appear on the structure. The reflectors are uniformly distributed on $l_k^{b,i} \in [-5, 5]$ and the position of each new reflector is Gaussian distributed $\mathcal{N}(l^{b,i}, \sigma_b^2)$, where $\sigma_b^2 = .75^2$ and the corresponding birth probability $P_{b,k}^i = \frac{0.1}{B_k}$. To reduce the computational complexity, the number of reflection centres on the structure is limited to four in this implementation. In our proposed filter we have a uniform clutter intensity set to $\mu = 0.1$ for all sensors, while in the vehicle tracking framework, the clutter intensity is estimated from data. The matrix, \mathbf{R}_u , that represents the sensor resolution in the resolution models is set based on the specified resolution cell, $[\delta_r, \delta_\phi, \delta_r]$, and is described in Section IV-C above and in Section IV-B in [3], respectively.

B. Tracking filter comparison

During the evaluated scenario, the side of the target vehicle is headed towards the host so that most measurements originate from features along that side, and consequently, the structure will adapt to represent the side of the target vehicle. This allows us to evaluate both lateral position and longitudinal extension together with the errors in angle and speed.

Figure 5 displays the absolute errors in lateral position, e_{lat} , heading angle, e_ψ , and speed, e_v . The error in lateral position is calculated as the mean distance between the reference vehicle side and the estimated side, i.e., the line structure or the estimated position of the side in the vehicle model. For the

most part, it is shown that the errors using our framework are similar as for the reference vehicle tracking framework. The main difference is found in e_v at $t \in [3, 6]s$ which is when the target slows down until standstill. Because of the low observability of the velocity, this is not clearly captured in the measurements. This situation causes problem for our model due to the uncertainties regarding the number and the positions of the reflection centres on the structure. The model thus needs to determine whether a received measurement originates from

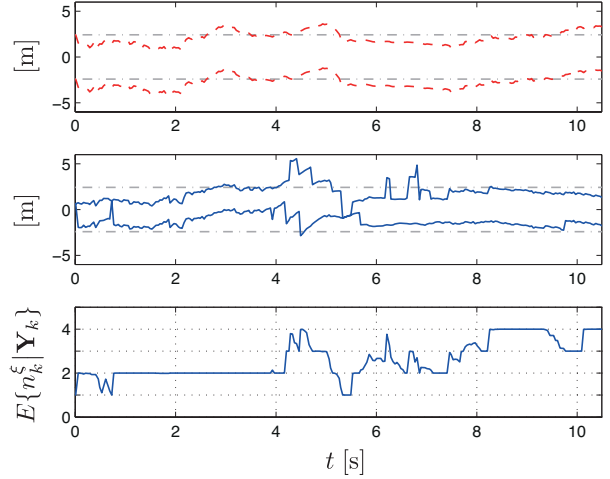


Figure 6. The top figure shows the estimated front and rear (dashed lines) using the vehicle tracking framework and the grey dashed lines shows the front and rear of the reference vehicle. The middle figure shows the same estimates for our proposed framework (solid line) while the bottom figure shows the expected number of reflector centres on the structure.

a reflection centre already on the structure or if a new reflector has become visible, and as a result, the model may add new reflectors to the structure instead of changing the velocity. However, as measurements are received while the target is stationary, the structure model recovers and the speed errors again resemble the ones for the reference vehicle tracking framework.

There are no obvious measures for evaluating how well the models describe the vehicle, since the object size is not included in our model but is a given parameter in the vehicle model. Nevertheless, to get an idea of how the structure model behaves, we compare the longitudinal extension of the two object models to the reference vehicle. The extension of the structure is here defined as the largest distance between any two reflectors, without taking into account the uncertainty regarding which reflectors that exist. Figure 6 shows the estimated front and rear positions of the vehicle side, using the vehicle tracking model (top) and the structure model (middle). The positions of the front and rear of the reference vehicle are indicated by the dashed grey lines in both cases. The bottom figure shows the expected number of reflection centres on the structure, $E\{n_k^\xi | \mathbf{Y}_k\}$, and it is worth noting that the structure in this implementation is limited to have at most four reflectors. During $t \in [2, 4]s$, it is clearly illustrated how the structure moves along the reference vehicle as it starts to break which causes an increase in the absolute speed error. An additional increase in e_v , and also a longitudinal error, occur after approximately 4.2 s as the structure adapts to some clutter measurements ahead of the vehicle. This is shown by the peak in the upper blue curve which clearly exceeds the reference front, and is also seen in the expected number of reflectors which increases at this time. The figures also show how the structure drops reflectors at $t \in [4.5, 5]s$ when it no longer accurately describes the received measurements. After that, it starts to recover and as the target gets closer

to the host and generates more measurements, the number of reflectors increases and the structure is covering almost the whole side of the reference. At two times in $t \in [6, 7]s$ the structure again adapts to clutter in front of the vehicle, which temporarily causes a longitudinal error. However, the probabilities of existence of these new reflectors soon get low and the reflectors are pruned.

VIII. CONCLUSION

In this paper we have presented a Bayesian filter framework for tracking an extended object using radar measurements. The object is modelled as a set of reflection centres on a line structure. The position of the object and the reflection centres are estimated recursively from data. This includes both estimating the number of reflectors and their positions. Moreover, the filter framework incorporates a radar sensor model that treats the limited sensor resolution and describes unresolved measurements from an arbitrary number of reflection centres.

The tracking framework has been evaluated using real radar data from an automotive scenario, and for reference we used the vehicle tracking framework in [3]. In contrast to our proposed model, the object size is known in the reference model, and conditioned on the state, the number of reflection centres and their positions are deterministic. For most parts, the evaluation shows similar results for the two models even though our model must use the received radar data to learn about the object. At a few occasions, it shows that our adaptive model is more sensitive to clutter than the reference model. That is when the structure adapts to clutter that is interpreted as a new reflection centre that has become visible.

APPENDIX A

There are two parts to the reflector model in (9): the deterministic positions of the reflectors in measurement space, \mathbf{r}_k , and a stochastic model of received signal amplitudes, σ_k . In this section we present these two parts separately, starting with the reflector positions.

A. Reflector model

To formulate \mathbf{r}_k^i , we start by finding the position of the reflector and the sensor in global Cartesian coordinates. The i^{th} reflection centre is positioned on the structure \mathbf{z}_k at an offset l_k^i from the rotation centre and, as a result, its global position is given as

$$\begin{bmatrix} x_k^i \\ y_k^i \end{bmatrix} = \begin{bmatrix} x_k \\ y_k \end{bmatrix} + l_k^i \begin{bmatrix} \cos(\psi_k + \theta_k) \\ \sin(\psi_k + \theta_k) \end{bmatrix}. \quad (94)$$

In addition, the velocity of the reflection centre has two components, one from the global velocity of the structure, $v_v^i = v_k$ in the ψ_k direction, and one from the rotation of the structure, $v_\perp^i = v_k c_k l_k^i$ in the $\pi - (\psi_k + \theta_k)$ direction.

The global position of the host platform is described by the known host state,

$$\mathbf{z}_k^h = [x_k^h, y_k^h, v_k^h, \psi_k^h, c_k^h]^T \quad (95)$$

on which a sensor, m , is mounted at $\mathbf{p}_s^m = [x_s^m, y_s^m]^T$ with an mounting angle of ψ_s^m . The global position of the sensor can, hence, be written as

$$\begin{bmatrix} x_k^s \\ y_k^s \end{bmatrix} = \begin{bmatrix} x_k^h \\ y_k^h \end{bmatrix} + \mathbf{R}(\psi_k^{ego}) \begin{bmatrix} x_s^m \\ y_s^m \end{bmatrix}. \quad (96)$$

From (94) and (96), the relative azimuth angle between sensor m and reflector centre i is found as

$$\alpha_{i,s} = \arg \left(\begin{bmatrix} x_k^i - x_k^s \\ y_k^i - y_k^s \end{bmatrix} \right). \quad (97)$$

The velocity component of the reflector in this direction (range rate) is given as

$$\dot{r}_k^r = \left(v_k \cos(\psi_k - \alpha_{i,s}) + v_\perp \cos\left(\frac{\pi}{2} + \psi_k + \theta_k - \alpha_{i,s}\right) \right) \quad (98)$$

and for the host platform

$$\dot{r}_k^h = \left(v_k^h \cos(\psi_k^h - \alpha_{i,s}) + v_\perp^h \cos\left(\frac{\pi}{2} + \arg(\mathbf{x}_s) - \alpha_{i,s}\right) \right) \quad (99)$$

where $v_\perp = v_k^h c_k^h \|\mathbf{p}_s^m\|$ is the velocity component due to rotation of the host platform.

The position of the i^{th} reflector in each dimension of the measurement space of sensor s can now be expressed as

$$\mathbf{r}_k^i = \begin{bmatrix} \sqrt{(x_k^i - x_k^s)^2 + (y_k^i - y_k^s)^2} \\ \alpha_{i,s} - \psi_k^h - \psi_s^m \\ \dot{r}_k^r - \dot{r}_k^h \end{bmatrix}. \quad (100)$$

B. Signal amplitude

The expected signal power of a reflector is characterised by two known functions, the angle dependent reciprocal antenna gain pattern, $g_\phi^s(\cdot)$, and the range dependent signal attenuation, $g_r^s(\cdot)$. Using these models, the expected return amplitude of reflector i is calculated as,

$$\sigma_k^i = g_\phi^s(\mathbf{r}_k^i) g_r^s(\mathbf{r}_k^i) \sigma_{rcs}, \quad (101)$$

where σ_{rcs} is the expected radar cross section of a reflector which is assumed to be known and constant. Furthermore, it is assumed that the functions, $g_\phi^s(\cdot)$ and $g_r^s(\cdot)$, are locally constant. As a result, the probability of detecting reflector i , determined by $\Pr\{A_k^i > \gamma_A\}$, is assumed to be locally state independent.

REFERENCES

- [1] S. Blackman and R. Popoli, *Design and analysis of modern tracking systems*. Norwood, MA: Artech House, 1999.
- [2] Y. Bar-Shalom and W. D. Blair, *Multitarget-Multisensor Tracking Volume III: Applications and Advances*. Norwood, MA: Artech House, 2000.
- [3] J. Gunnarsson, L. Svensson, L. Danielsson, and F. Bengtsson, “Tracking vehicles using radar detections,” in *Intelligent Vehicles Symposium, 2007. Proceedings IEEE*, Istanbul, June 2007.
- [4] R. Ostrovityanov and F. Basalov, *Statistical Theory of Extended Radar Targets*. Artech House, 1985.
- [5] F. E. Daum and R. J. Fitzgerald, “Importance of resolution in multiple-target tracking,” *Signal and Data Processing of Small Targets 1994*, vol. 2235, no. 1, pp. 329–338, 1994. [Online]. Available: <http://link.aip.org/link/?PSI/2235/329/1>

- [6] M. Waxman and O. Drummond, "A bibliography of cluster (group) tracking," in *Signal and Data Processing of Small Targets 2004. Edited by Drummond, Oliver E. Proceedings of the SPIE*, vol. 5428, 2004, pp. 551–560.
- [7] R. Mahler, "Multitarget Bayes filtering via first-order multitarget moments," *Aerospace and Electronic Systems, IEEE Transactions on*, vol. 39, no. 4, pp. 1152–1178, 2004.
- [8] ———, "Multitarget bayes filtering via first-order multitarget moments," *Aerospace and Electronic Systems, IEEE Transactions on*, vol. 39, no. 4, pp. 1152–1178, 2003.
- [9] K. Granstrom, C. Lundquist, and U. Orguner, "A gaussian mixture phd filter for extended target tracking," in *Information Fusion (FUSION), 2010 13th Conference on*, 2010, pp. 1–8.
- [10] J. Koch, "Bayesian approach to extended object and cluster tracking using random matrices," *Aerospace and Electronic Systems, IEEE Transactions on*, vol. 44, no. 3, pp. 1042–1059, 2008.
- [11] W. Koch, "Advanced sensor models: Benefits for target tracking and sensor data fusion," in *Multisensor Fusion and Integration for Intelligent Systems, 2006 IEEE International Conference on*, sep 2006, pp. 565–570.
- [12] M. Baum and U. Hanebeck, "Extended object tracking based on combined set-theoretic and stochastic fusion," in *Information Fusion, 2009. FUSION '09. 12th International Conference on*, 2009, pp. 1288–1295.
- [13] T. Broda and R. Chellappa, "Estimating the kinematics and structure of a rigid object from a sequence of monocular images," *IEEE Transactions on Pattern Analysis and Machine Intelligence*, vol. 13, no. 6, pp. 497–513, 1991.
- [14] T. Huang and A. Netravali, "Motion and structure from feature correspondences: A review," *Advances in image processing and understanding: a festschrift for Thomas S. Huang*, p. 331, 2002.
- [15] J. Dezert, "Tracking maneuvering and bending extended target in cluttered environment," in *Proceedings of SPIE*, vol. 3373, 1998, p. 283.
- [16] D. Salmond and N. Gordon, "Group and extended object tracking," in *IEE Colloquium on Target Tracking: Algorithms and Applications (Ref. No. 1999/090, 1999/215)*, 1999, pp. 16/1–16/4.
- [17] K. Gilholm, S. J. Godsill, S. Maskell, and D. J. Salmond, "Poisson models for extended target and group tracking," *SPIE*, October 2005.
- [18] K.-C. Chang and Y. Bar-Shalom, "Joint probabilistic data association for multitarget tracking with possibly unresolved measurements and maneuvers," *Automatic Control, IEEE Transactions on*, vol. 29, no. 7, pp. 585–594, Jul 1984.
- [19] W. Koch and G. Van Keuk, "Multiple hypothesis track maintenance with possibly unresolved measurements," *Aerospace and Electronic Systems, IEEE Transactions on*, vol. 33, no. 3, pp. 883–892, July 1997.
- [20] D. Svensson, M. Ulmke, and L. Danielsson, "Multi-target sensor resolution model for arbitrary target numbers," in *Proceedings of SPIE Signal and Data Processing of Small Targets 2010*, April 2010.
- [21] N. Gordon, D. Salmond, and D. Fisher, "Bayesian target tracking after group pattern distortion," in *Proceedings of SPIE*, vol. 3163, 1997, p. 238.
- [22] P. Swerling, "Probability of detection for fluctuating targets," *Information Theory, IRE Transactions on*, vol. 6, no. 2, pp. 269–308, 1960.
- [23] T. Fortmann, Y. Bar-Shalom, and M. Scheffe, "Sonar tracking of multiple targets using joint probabilistic data association," *IEEE Journal of Oceanic Engineering*, vol. 8, July 1983.
- [24] S. Julier and J. Uhlmann, "Unscented filtering and nonlinear estimation," *Proceedings of the IEEE*, vol. 92, no. 3, pp. 401 – 22, 2004.
- [25] P. Ainsleigh, N. Kehtarnavaz, and R. Streit, "Hidden Gauss-Markov models for signal classification," *IEEE Transactions on Signal Processing*, vol. 50, no. 6, pp. 1355–1367, 2002.
- [26] D. Salmond, "Mixture reduction algorithms for target tracking in clutter," in *Proceedings of SPIE*, vol. 1305, 1990, p. 434.



Lars Hammarstrand was born in Landvetter, Sweden in 1979. He received his M.Sc. and Ph.D. degree in electrical engineering from Chalmers University of Technology, Gothenburg, Sweden, in 2004 and 2010, respectively.

He is currently with the Active Safety and Chassis Department at Volvo Car Corporation, Gothenburg responsible for sensor data fusion developments. His main research interests are in the fields of sensor fusion and radar sensor modeling, especially with application to active safety systems.



Malin Lundgren was born in Skövde, Sweden in 1979. She received the M.Sc. degree in Electrical Engineering from Chalmers University of Technology, Göteborg, Sweden, in 2004. After a couple of years in the industry she returned to Chalmers where she is currently working as a Ph.D. student with interest in sensor fusion and extended object tracking, primarily for automotive safety applications.



Lennart Svensson was born in Älvängen, Sweden in 1976. He received the M.S. degree in electrical engineering in 1999 and the Ph.D. degree in 2004, both from Chalmers University of Technology, Gothenburg, Sweden.

He is currently an Associate Professor at the Signal Processing group, again at Chalmers University of Technology. His research interests include Bayesian inference in general, and nonlinear filtering and tracking in particular.